Collider sensitivity to SMEFT heavy-quark operators at one-loop in top-quark processes

LHC EFT WG - 7th General Meeting

Andres Vasquez, Celine Degrande, Rogerio Rosenfeld

Based on arXiv: 2402.06528 (hep-ph)

Geneva, April 24th - 2024

universitätbonn bctp

UCLouvain
Institut de recherche
en mathématique et physique

IFT - UNESP
INSTITUTO DE FÍSICA TEÓRICA

Motivation

- No clear evidence for new physics from direct searches.
- LHC is reaching a precision era.
- Systematic uncertainties start to dominate in several situations.

→ This demands high precision in theoretical predictions.

Complementary approach: Standard Model Effective Field Theory

Going NLO

Ultimate goal: Precision global fit of the full SMEFT based on LHC observables.

Obtain SMEFT predictions to the precision level of the LHC.

Motivation

- No clear evidence for new physics from direct searches.
- LHC is reaching a precision era.
- Systematic uncertainties start to dominate in several situations.

→ This demands high precision in theoretical predictions.

Complementary approach: Standard Model Effective Field Theory

Going NLO

Ultimate goal: Precision global fit of the full SMEFT based on LHC observables.

Obtain SMEFT predictions to the precision level of the LHC.

We focus on deviations parametrised by four-fermion interactions involving four top quarks.

They should appear as soon as new physics couples to the top quark.

In this work we explored the effects of four top quark operators at NLO in the top-pair production

SMEFT

The SMEFT is a model-independent parametrization of deviations from the SM. The Lagrangian is given by,

$$\mathscr{L}_{\text{SMEFT}} = \mathscr{L}_{\text{SM}} + \sum_{i,d>4} \frac{c_i^{(d)}(\mu)}{\Lambda^{d-4}} \mathcal{O}_i^{(d)}$$

With the c_i indicating the Wilson coefficients and Λ the new cutoff energy.

This low-energy theory:

- is based on the SM fields only,
- respects the symmetries of the SM,
- must be used below the cutoff.

From this follows that the SMEFT is self-consistent, gauge invariant and renormalizable order by order in $1/\Lambda$.

SMEFT

The SMEFT is a model-independent parametrization of deviations from the SM. The Lagrangian is given by,

$$\mathscr{L}_{\text{SMEFT}} = \mathscr{L}_{\text{SM}} + \sum_{i,d>4} \frac{c_i^{(d)}(\mu)}{\Lambda^{d-4}} \mathscr{O}_i^{(d)}$$

With the c_i indicating the Wilson coefficients and Λ the new cutoff energy.

This low-energy theory:

- is based on the SM fields only,
- respects the symmetries of the SM,
- must be used below the cutoff.

From this follows that the SMEFT is self-consistent, gauge invariant and renormalizable order by order in $1/\Lambda$.

With this, parametrizations of possible deviations from the SM in the observable O_n are of the form

$$\Delta \mathrm{O}_n = \mathrm{O}_n^{\text{EXP}} - \mathrm{O}_n^{\text{SM}} = \sum_i \frac{a_{n,i}^{(6)}(\mu) c_i^{(6)}(\mu)}{\Lambda^2} + \sum_{ij} \frac{b_{n,ij}^{(6)}(\mu) c_i^{(6)}(\mu) c_j^{(6)}(\mu)}{\Lambda^4} + \sum_i \frac{a_{n,i}^{(8)}(\mu) c_i^{(8)}(\mu)}{\Lambda^4} + \dots$$

EFT operators

$(\bar{L}L)(\bar{L}L)$		$(\bar{R}R)(\bar{R}R)$		$(\bar{L}L)(\bar{R}R)$	
Q_{ll}	$(\bar{l}_p\gamma_\mu l_r)(\bar{l}_s\gamma^\mu l_t)$	Q_{ee}	$(\bar{e}_p\gamma_\mu e_r)(\bar{e}_s\gamma^\mu e_t)$	Q_{le}	$(\bar{l}_p\gamma_\mu l_r)(\bar{e}_s\gamma^\mu e_t)$
$Q_{qq}^{(1)}$	$(\bar{q}_p\gamma_\mu q_r)(\bar{q}_s\gamma^\mu q_t)$	Q_{uu}	$(\bar{u}_p\gamma_\mu u_r)(\bar{u}_s\gamma^\mu u_t)$	Q_{lu}	$(\bar{l}_p\gamma_\mu l_r)(\bar{u}_s\gamma^\mu u_t)$
$Q_{qq}^{(3)}$	$(\bar{q}_p\gamma_\mu\tau^I q_r)(\bar{q}_s\gamma^\mu\tau^I q_t)$	Q_{dd}	$(\bar{d}_p\gamma_\mu d_r)(\bar{d}_s\gamma^\mu d_t)$	Q_{ld}	$(\bar{l}_p\gamma_\mu l_r)(\bar{d}_s\gamma^\mu d_t)$
$Q_{lq}^{(1)}$	$(\bar{l}_p\gamma_\mu l_r)(\bar{q}_s\gamma^\mu q_t)$	Q_{eu}	$(\bar{e}_p\gamma_\mu e_r)(\bar{u}_s\gamma^\mu u_t)$	Q_{qe}	$(\bar{q}_p\gamma_\mu q_r)(\bar{e}_s\gamma^\mu e_t)$
$Q_{lq}^{(3)}$	$(\bar{l}_p\gamma_\mu\tau^I l_r)(\bar{q}_s\gamma^\mu\tau^I q_t)$	Q_{ed}	$(\bar{e}_p\gamma_\mu e_r)(\bar{d}_s\gamma^\mu d_t)$	$Q_{qu}^{(1)}$	$(\bar{q}_p\gamma_\mu q_r)(\bar{u}_s\gamma^\mu u_t)$
		$Q_{ud}^{(1)}$	$(\bar{u}_p\gamma_\mu u_r)(\bar{d}_s\gamma^\mu d_t)$	$Q_{qu}^{(8)}$	$(\bar{q}_p\gamma_\mu T^A q_r)(\bar{u}_s\gamma^\mu T^A u_t)$
		$Q_{ud}^{(8)}$	$(\bar{u}_p\gamma_\mu T^A u_r)(\bar{d}_s\gamma^\mu T^A d_t)$	$Q_{qd}^{(1)}$	$(\bar{q}_p\gamma_\mu q_r)(\bar{d}_s\gamma^\mu d_t)$
				$Q_{qd}^{(8)}$	$(\bar{q}_p\gamma_\mu T^A q_r)(\bar{d}_s\gamma^\mu T^A d_t)$

In this work we focus on the four-heavy-quark operators

$$\mathcal{O}_{Qt}^{(1)} = (\bar{Q}_L\gamma_\mu Q_L)\,(\bar{t}_R\gamma^\mu t_R)\,, \qquad \mathcal{O}_{Qt}^{(8)} = (\bar{Q}_L\gamma_\mu T^A Q_L)\,(\bar{t}_R\gamma^\mu T^A t_R)\,,$$

$$\mathcal{O}_{QQ}^{(1)} = \frac{1}{2}\,(\bar{Q}_L\gamma_\mu Q_L)\,(\bar{Q}_L\gamma^\mu Q_L)\,, \quad \mathcal{O}_{QQ}^{(8)} = \frac{1}{2}\,(\bar{Q}_L\gamma_\mu T^A Q_L)\,(\bar{Q}_L\gamma^\mu T^A Q_L)\,,$$

$$\mathcal{O}_{tt}^{(1)} = (\bar{t}_R\gamma_\mu t_R)\,(\bar{t}_R\gamma^\mu t_R)\,.$$

EFT operators

$(\bar{L}L)(\bar{L}L)$		$(\bar{R}R)(\bar{R}R)$		$(\bar{L}L)(\bar{R}R)$	
Q_{ll}	$(\bar{l}_p\gamma_\mu l_r)(\bar{l}_s\gamma^\mu l_t)$	Q_{ee}	$(\bar{e}_p\gamma_\mu e_r)(\bar{e}_s\gamma^\mu e_t)$	Q_{le}	$(\bar{l}_p\gamma_\mu l_r)(\bar{e}_s\gamma^\mu e_t)$
$Q_{qq}^{(1)}$	$(\bar{q}_p\gamma_\mu q_r)(\bar{q}_s\gamma^\mu q_t)$	Q_{uu}	$(\bar{u}_p\gamma_\mu u_r)(\bar{u}_s\gamma^\mu u_t)$	Q_{lu}	$(\bar{l}_p\gamma_\mu l_r)(\bar{u}_s\gamma^\mu u_t)$
$Q_{qq}^{(3)}$	$(\bar{q}_p\gamma_\mu \tau^I q_r)(\bar{q}_s\gamma^\mu \tau^I q_t)$	Q_{dd}	$(\bar{d}_p\gamma_\mu d_r)(\bar{d}_s\gamma^\mu d_t)$	Q_{ld}	$(\bar{l}_p\gamma_\mu l_r)(\bar{d}_s\gamma^\mu d_t)$
$Q_{lq}^{(1)}$	$(\bar{l}_p\gamma_\mu l_r)(\bar{q}_s\gamma^\mu q_t)$	Q_{eu}	$(\bar{e}_p\gamma_\mu e_r)(\bar{u}_s\gamma^\mu u_t)$	Q_{qe}	$(\bar{q}_p\gamma_\mu q_r)(\bar{e}_s\gamma^\mu e_t)$
$Q_{lq}^{(3)}$	$(\bar{l}_p\gamma_\mu \tau^I l_r)(\bar{q}_s\gamma^\mu \tau^I q_t)$	Q_{ed}	$(\bar{e}_p\gamma_\mu e_r)(\bar{d}_s\gamma^\mu d_t)$	$Q_{qu}^{(1)}$	$(\bar{q}_p\gamma_\mu q_r)(\bar{u}_s\gamma^\mu u_t)$
		$Q_{ud}^{(1)}$	$(\bar{u}_p\gamma_\mu u_r)(\bar{d}_s\gamma^\mu d_t)$	$Q_{qu}^{(8)}$	$(\bar{q}_p\gamma_\mu T^A q_r)(\bar{u}_s\gamma^\mu T^A u_t)$
		$Q_{ud}^{(8)}$	$(\bar{u}_p\gamma_\mu T^A u_r)(\bar{d}_s\gamma^\mu T^A d_t)$	$Q_{qd}^{(1)}$	$(\bar{q}_p\gamma_\mu q_r)(\bar{d}_s\gamma^\mu d_t)$
				$Q_{qd}^{(8)}$	$(\bar{q}_p\gamma_\mu T^A q_r)(\bar{d}_s\gamma^\mu T^A d_t)$

In this work we focus on the four-heavy-quark operators

$$\mathcal{O}_{Qt}^{(1)} = (\bar{Q}_L\gamma_\mu Q_L)\,(\bar{t}_R\gamma^\mu t_R)\,, \qquad \mathcal{O}_{Qt}^{(8)} = (\bar{Q}_L\gamma_\mu T^A Q_L)\,(\bar{t}_R\gamma^\mu T^A t_R)\,,$$
$$\mathcal{O}_{QQ}^{(1)} = \frac{1}{2}\,(\bar{Q}_L\gamma_\mu Q_L)\,(\bar{Q}_L\gamma^\mu Q_L)\,, \quad \mathcal{O}_{QQ}^{(8)} = \frac{1}{2}\,(\bar{Q}_L\gamma_\mu T^A Q_L)\,(\bar{Q}_L\gamma^\mu T^A Q_L)\,,$$
$$\mathcal{O}_{tt}^{(1)} = (\bar{t}_R\gamma_\mu t_R)\,(\bar{t}_R\gamma^\mu t_R)\,.$$

Vertices:

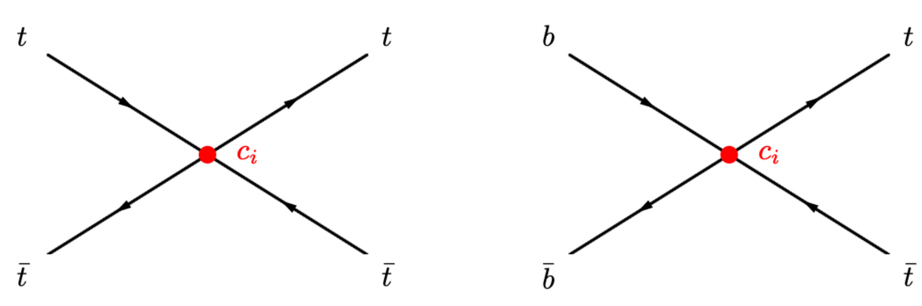

All of these operators enter at tree level in the four-top process and at one-loop in the top-pair production.

State of the Art

EWPO and Higgs related observables can impose bounds on some subsets of these five operators.

EWPO:

[Dawson & Giardino, 2022]

through the observables $\Gamma_Z,\ \sigma_{\mathrm{h}},\ R_l,\ R_b,\ R_c,\ A_b, A_{b,\mathrm{FB}}$

via corrections

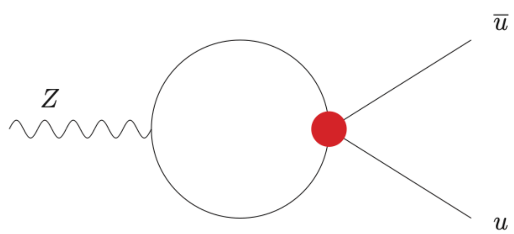

Constraints on

$$\mathcal{O}_{QQ}^{(1)} = \frac{1}{2}\left(\bar{Q}_L\gamma_\mu Q_L\right)\left(\bar{Q}_L\gamma^\mu Q_L\right),$$
$$\mathcal{O}_{QQ}^{(8)} = \frac{1}{2}\left(\bar{Q}_L\gamma_\mu T^A Q_L\right)\left(\bar{Q}_L\gamma^\mu T^A Q_L\right),$$
$$\mathcal{O}_{Qt}^{(1)} = \left(\bar{Q}_L\gamma_\mu Q_L\right)\left(\bar{t}_R\gamma^\mu t_R\right)$$

$\longrightarrow$

$$c_{QQ}^{1} \in [-1.61, 2.68],$$
$$c_{QQ}^{8} \in [-15.23, 25.41],$$
$$c_{Qt}^{1} \in [-2.24, 1.35]$$

State of the Art

EWPO and Higgs related observables can impose bounds on some subsets of these five operators.

EWPO:

through the observables $\Gamma_Z,\ \sigma_{\mathrm{h}},\ R_l,\ R_b,\ R_c,\ A_b,\ A_{b,\mathrm{FB}}$

via corrections

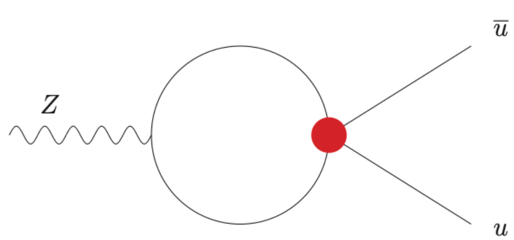

[Dawson & Giardino, 2022]

Constraints on

$$\mathcal{O}^{(1)}_{QQ} = \frac{1}{2}\left(\bar{Q}_L\gamma_\mu Q_L\right)\left(\bar{Q}_L\gamma^\mu Q_L\right),$$
$$\mathcal{O}^{(8)}_{QQ} = \frac{1}{2}\left(\bar{Q}_L\gamma_\mu T^A Q_L\right)\left(\bar{Q}_L\gamma^\mu T^A Q_L\right),$$
$$\mathcal{O}^{(1)}_{Qt} = \left(\bar{Q}_L\gamma_\mu Q_L\right)\left(\bar{t}_R\gamma^\mu t_R\right)$$

$\longrightarrow$

$$c^1_{QQ} \in [-1.61, 2.68],$$
$$c^8_{QQ} \in [-15.23, 25.41],$$
$$c^1_{Qt} \in [-2.24, 1.35]$$

Higgs processes:

[Alasfar, de Blas & Gröber, 2022]

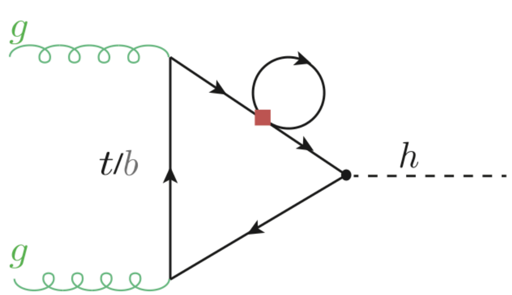

Gluon-Fusion
Higgs production

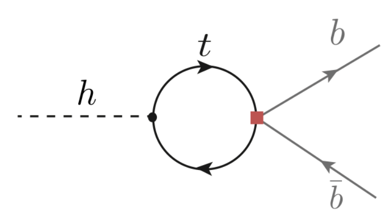

Higgs decay

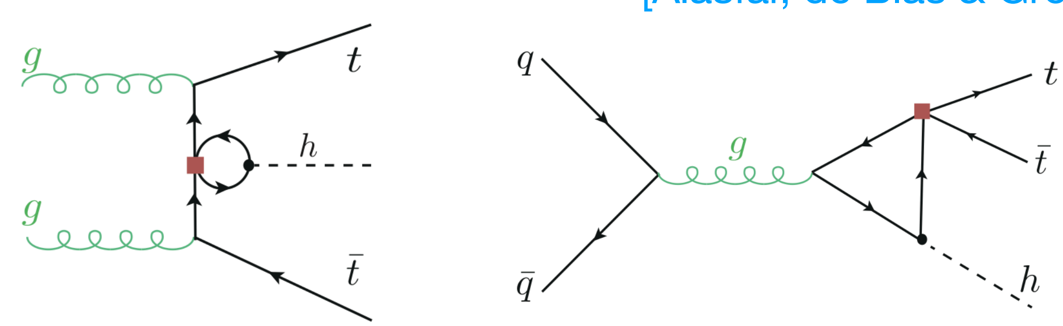

Higgs production
in association with ttbar

State of the Art

EWPO and Higgs related observables can impose bounds on some subsets of these five operators.

EWPO:

through the observables $\Gamma_Z,\ \sigma_\mathrm{h},\ R_l,\ R_b,\ R_c,\ A_b,\ A_{b,\mathrm{FB}}$

via corrections

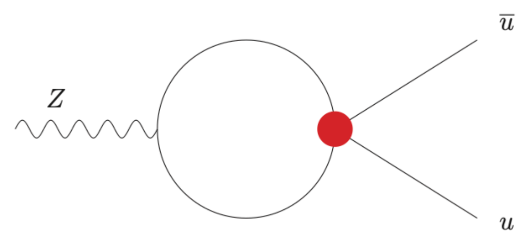

[Dawson & Giardino, 2022]

Constraints on

$$\mathcal{O}^{(1)}_{QQ} = \frac{1}{2}\left(\bar{Q}_L\gamma_\mu Q_L\right)\left(\bar{Q}_L\gamma^\mu Q_L\right),$$
$$\mathcal{O}^{(8)}_{QQ} = \frac{1}{2}\left(\bar{Q}_L\gamma_\mu T^A Q_L\right)\left(\bar{Q}_L\gamma^\mu T^A Q_L\right),$$
$$\mathcal{O}^{(1)}_{Qt} = \left(\bar{Q}_L\gamma_\mu Q_L\right)\left(\bar{t}_R\gamma^\mu t_R\right)$$

$$c^1_{QQ} \in [-1.61, 2.68],$$
$$c^8_{QQ} \in [-15.23, 25.41],$$
$$c^1_{Qt} \in [-2.24, 1.35]$$

Higgs processes:

Constraints on

$$\mathcal{O}^{(8)}_{Qt} = \left(\bar{Q}_L\gamma_\mu T^A Q_L\right)\left(\bar{t}_R\gamma^\mu T^A t_R\right),$$
$$\mathcal{O}^{(1)}_{Qt} = \left(\bar{Q}_L\gamma_\mu Q_L\right)\left(\bar{t}_R\gamma^\mu t_R\right)$$

Gluon-Fusion
Higgs production

Higgs decay

Sizeable constraints only via ttH for operators with mixed chiralities.

$$c^1_{Qt} \in [-1.1, 1.2],$$
$$c^8_{Qt} \in [-4.6, 4.9],$$

[Alasfar, de Blas & Gröber, 2022]

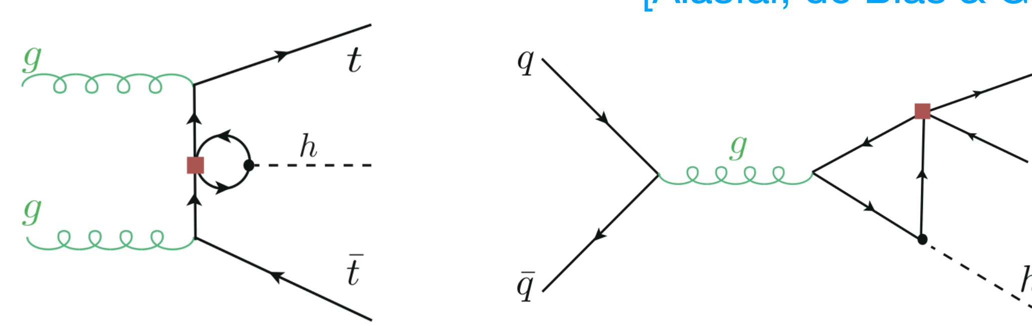

Higgs production
in association with ttbar

State of the Art

EWPO and Higgs related observables can impose bounds on some subsets of these five operators.

EWPO:

through the observables $\Gamma_Z,\ \sigma_{\mathrm{h}},\ R_l,\ R_b,\ R_c,\ A_b,\ A_{b,\mathrm{FB}}$

via corrections

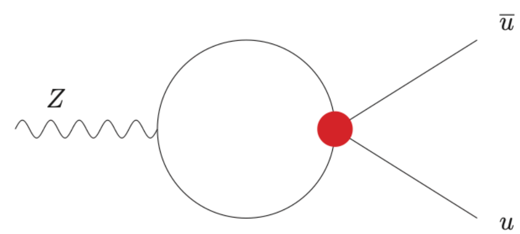

[Dawson & Giardino, 2022]

Constraints on

$$\mathcal{O}^{(1)}_{QQ} = \frac{1}{2}\left(\bar{Q}_L\gamma_\mu Q_L\right)\left(\bar{Q}_L\gamma^\mu Q_L\right),$$
$$\mathcal{O}^{(8)}_{QQ} = \frac{1}{2}\left(\bar{Q}_L\gamma_\mu T^A Q_L\right)\left(\bar{Q}_L\gamma^\mu T^A Q_L\right),$$
$$\mathcal{O}^{(1)}_{Qt} = \left(\bar{Q}_L\gamma_\mu Q_L\right)\left(\bar{t}_R\gamma^\mu t_R\right)$$

$\longrightarrow$

$$c^1_{QQ} \in [-1.61, 2.68],$$
$$c^8_{QQ} \in [-15.23, 25.41],$$
$$c^1_{Qt} \in [-2.24, 1.35]$$

Bounds from global fit combining $t\bar{t}t\bar{t}$ and $t\bar{t}b\bar{b}$

[SMEFiT collaboration, 2021]

Higgs processes:

Constraints on

$$\mathcal{O}^{(8)}_{Qt} = \left(\bar{Q}_L\gamma_\mu T^A Q_L\right)\left(\bar{t}_R\gamma^\mu T^A t_R\right),$$
$$\mathcal{O}^{(1)}_{Qt} = \left(\bar{Q}_L\gamma_\mu Q_L\right)\left(\bar{t}_R\gamma^\mu t_R\right)$$

Sizeable constraints only via ttH for operators with mixed chiralities.

$$c^1_{Qt} \in [-1.1, 1.2],$$
$$c^8_{Qt} \in [-4.6, 4.9],$$

[Alasfar, de Blas & Gröber, 2022]

Gluon-Fusion
Higgs production

Higgs decay

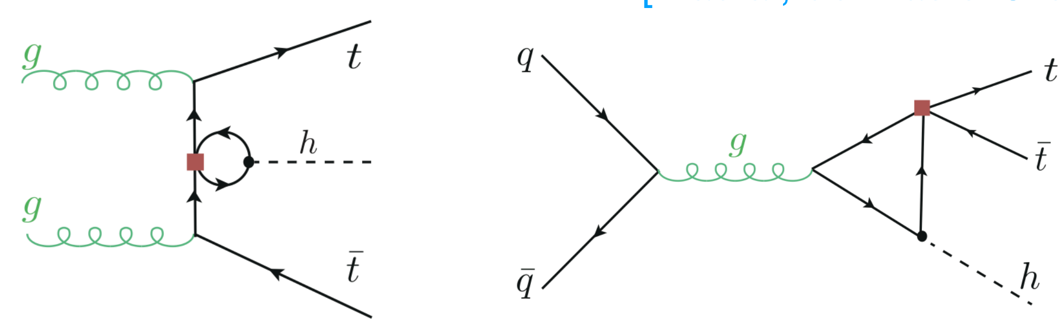

Higgs production
in association with ttbar

Four-Top production

The typical cross-section for this process is of some few fb, thus naively we could expect its constraining power not as large as those from other processes.

In reality, this is compensated by the high sensitivity of the $t\bar{t}t\bar{t}$ process to four-quark operators.

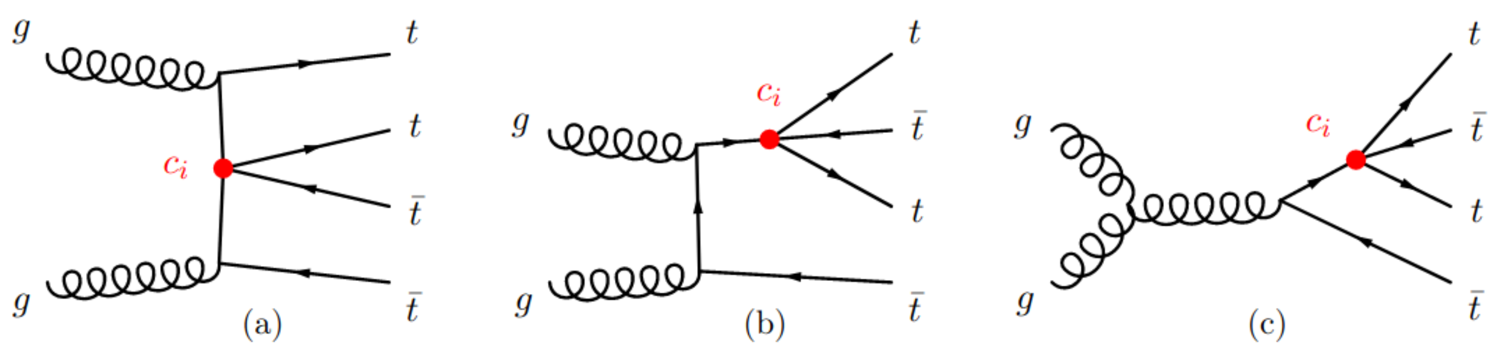

At the LHC with CoM energy of 13 TeV

$$\sigma_{\rm SM}(pp \to t\bar{t}t\bar{t}) \simeq 12 \text{ fb}$$

Four-Top production

The typical cross-section for this process is of some few fb, thus naively we could expect its constraining power not as large as those from other processes.

In reality, this is compensated by the high sensitivity of the $t\bar{t}t\bar{t}$ process to four-quark operators.

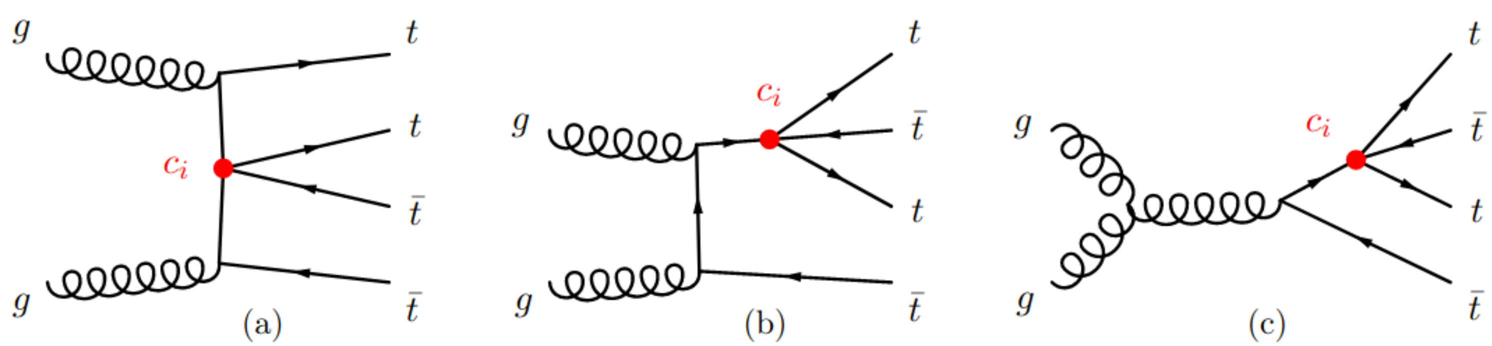

At the LHC with CoM energy of 13 TeV

$$\sigma_{\rm SM}(pp \to t\bar{t}t\bar{t}) \simeq 12 \text{ fb}$$

c_i	$\mathcal{O}(\Lambda^{-2})$			$\mathcal{O}(\Lambda^{-4})$
	$\mathcal{O}(\alpha_s^2\Lambda^{-2})$	$\mathcal{O}(\alpha_s\alpha\,\Lambda^{-2})$	Total interf.	
c^1_{tt}	$0.552^{+71\%}_{-39\%}$	-1.74	-1.24	$4.25^{+73\%}_{-39\%}$
c^1_{QQ}	$0.272^{+71\%}_{-39\%}$	-0.991	-0.737	$1.06^{+73\%}_{-39\%}$
c^8_{QQ}	$0.0889^{+71\%}_{-39\%}$	-0.329	-0.245	$0.118^{+73\%}_{-39\%}$
c^1_{Qt}	$-0.0392^{+71\%}_{-39\%}$	0.747	0.745	$1.44^{+73\%}_{-39\%}$
c^8_{Qt}	$0.282^{+70\%}_{-39\%}$	-0.605	-0.322	$0.349^{+73\%}_{-39\%}$

Values in fb

Related by a factor of 2 and 4, respectively

Due to a factor of 2 in the definitions

Four-Top production

The typical cross-section for this process is of some few fb, thus naively we could expect its constraining power not as large as those from other processes.

In reality, this is compensated by the high sensitivity of the $t\bar{t}t\bar{t}$ process to four-quark operators.

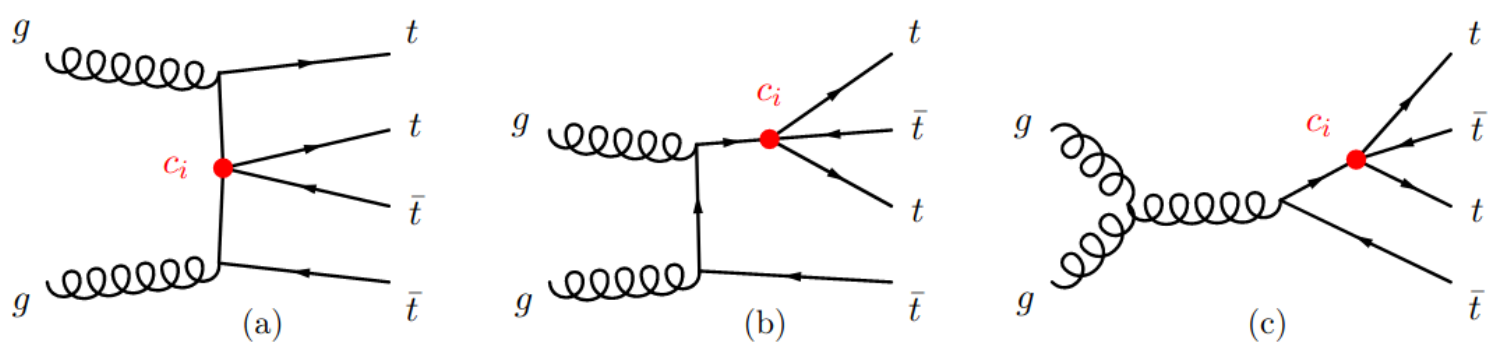

At the LHC with CoM energy of 13 TeV

$$\sigma_{\mathrm{SM}}(pp \to t\bar{t}t\bar{t}) \simeq 12 \text{ fb}$$

c_i	$\mathcal{O}(\Lambda^{-2})$			$\mathcal{O}(\Lambda^{-4})$
	$\mathcal{O}(\alpha_s^2\Lambda^{-2})$	$\mathcal{O}(\alpha_s\alpha\,\Lambda^{-2})$	Total interf.	
c_{tt}^1	$0.552^{+71\%}_{-39\%}$	-1.74	-1.24	$4.25^{+73\%}_{-39\%}$
c_{QQ}^1	$0.272^{+71\%}_{-39\%}$	-0.991	-0.737	$1.06^{+73\%}_{-39\%}$
c_{QQ}^8	$0.0889^{+71\%}_{-39\%}$	-0.329	-0.245	$0.118^{+73\%}_{-39\%}$
c_{Qt}^1	$-0.0392^{+71\%}_{-39\%}$	0.747	0.745	$1.44^{+73\%}_{-39\%}$
c_{Qt}^8	$0.282^{+70\%}_{-39\%}$	-0.605	-0.322	$0.349^{+73\%}_{-39\%}$

Values in fb

Related by a factor of 2 and 4, respectively

Due to a factor of 2 in the definitions

Related by a factor of 3 and 9, respectively

These are sources of degeneracy in the four-top production.

$$\mathcal{O}_{QQ}^{(8)} \overset{tttt\text{−only}}{=} \frac{1}{3}\mathcal{O}_{QQ}^{(1)}$$

Four-Top production

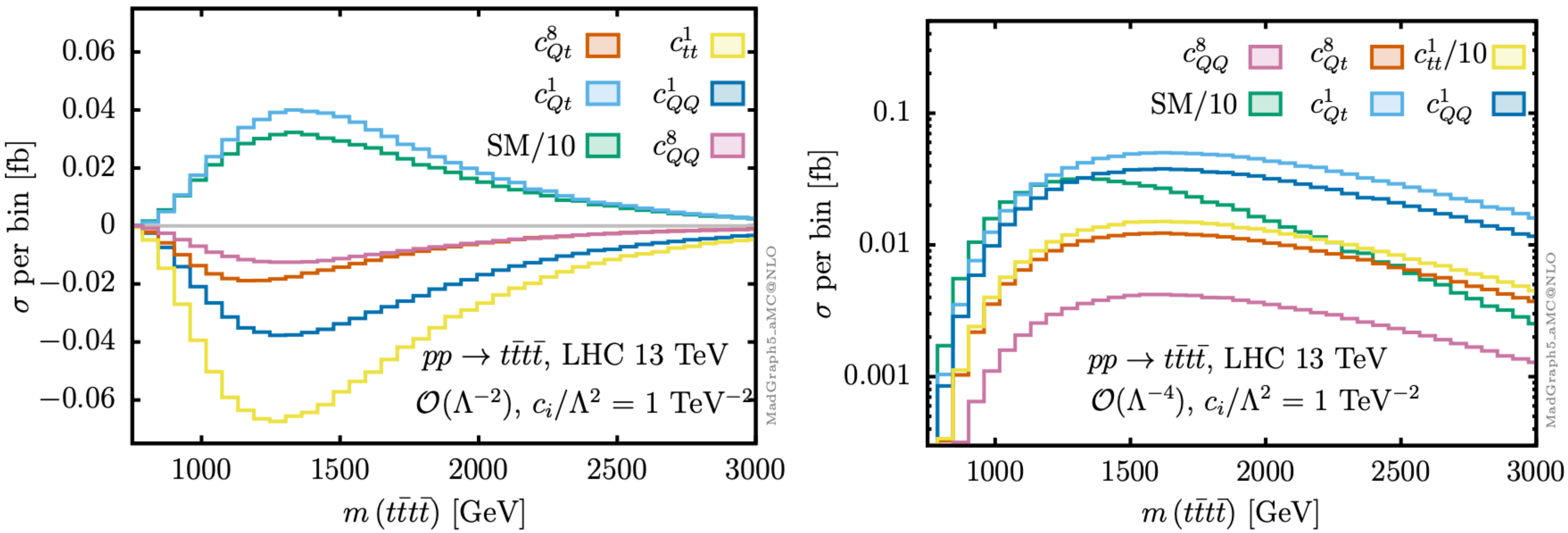

- The invariant mass distributions linear in the c_i present peaks at ~ 1.3 TeV.
- Square contributions dominate in the high-energy regime, presenting peaks at ~1.7 TeV. They also fall slower than the corresponding linear distribution.
- The shapes of the invariant mass distributions are very similar at high energy.

Four-Top production

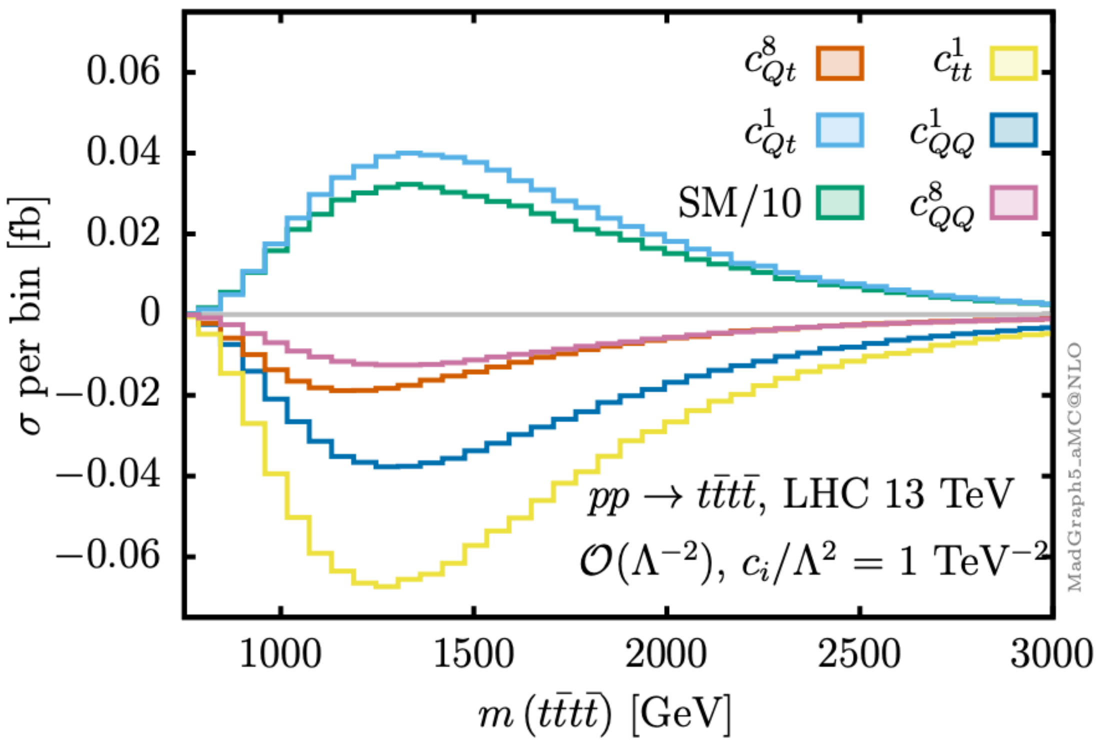

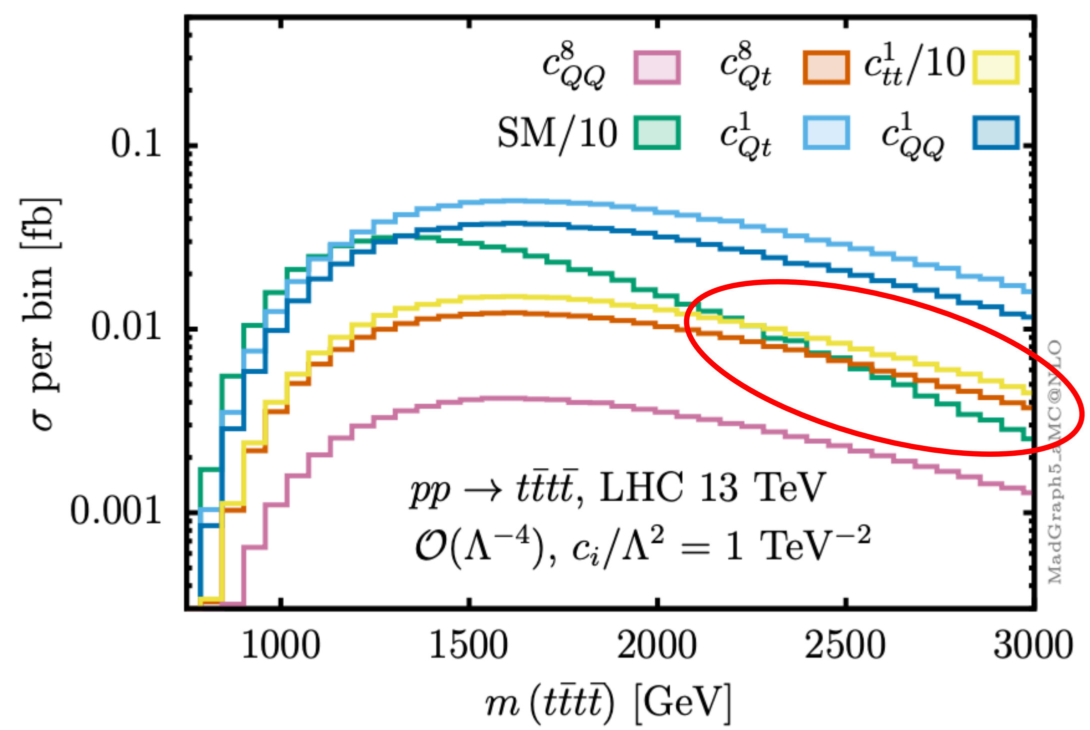

Worrisome region: SMEFT > SM
for $c_i/\Lambda^2\ 1\ \mathrm{TeV}^{-2}$

Impose severe cuts in the P.S. or
require stringent bounds to be valid

- The invariant mass distributions linear in the c_i present peaks at ~ 1.3 TeV.
- Square contributions dominate in the high-energy regime, presenting peaks at ~1.7 TeV. They also fall slower than the corresponding linear distribution.
- The shapes of the invariant mass distributions are very similar at high energy.

Top-pair production

The four-heavy-quark operators enter through the following diagrams

Quark induced channel

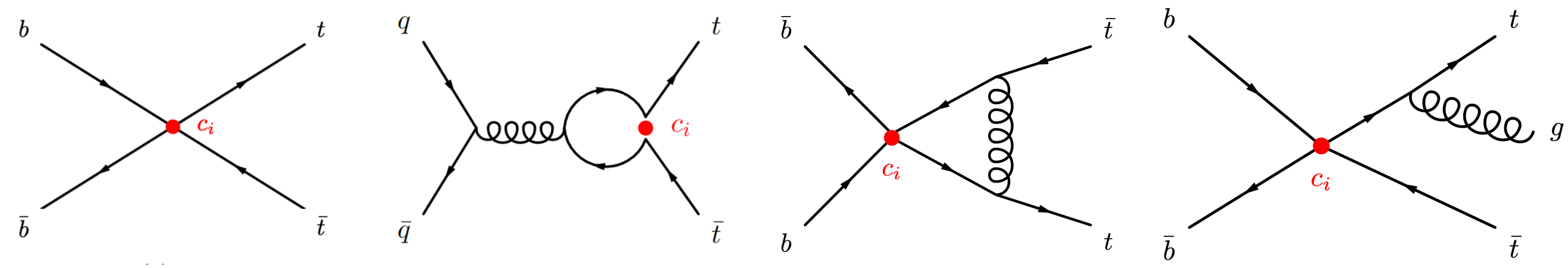

Gluon induced channel

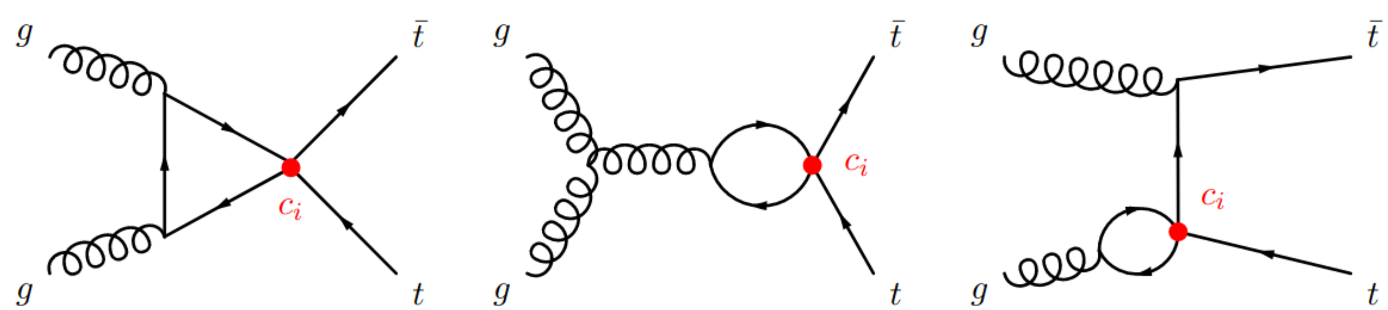

Observables are then computed as:

$$\mathrm{O}_{\mathrm{SMEFT}}\left(\frac{c_i}{\Lambda^2}\right) = \mathrm{O}_{\mathrm{SM}} + \sum_i a_i \frac{c_i}{\Lambda^2} + \sum_{ij} b_{ij} \frac{c_i c_j}{\Lambda^4}$$

Top-pair production

The four-heavy-quark operators enter through the following diagrams

Quark induced channel

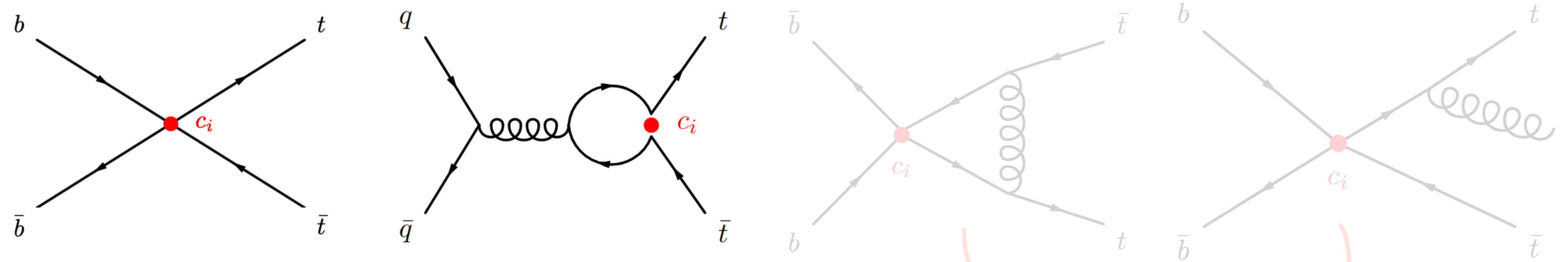

Suppressed by loop factor and bottom quark PDFs

Gluon induced channel

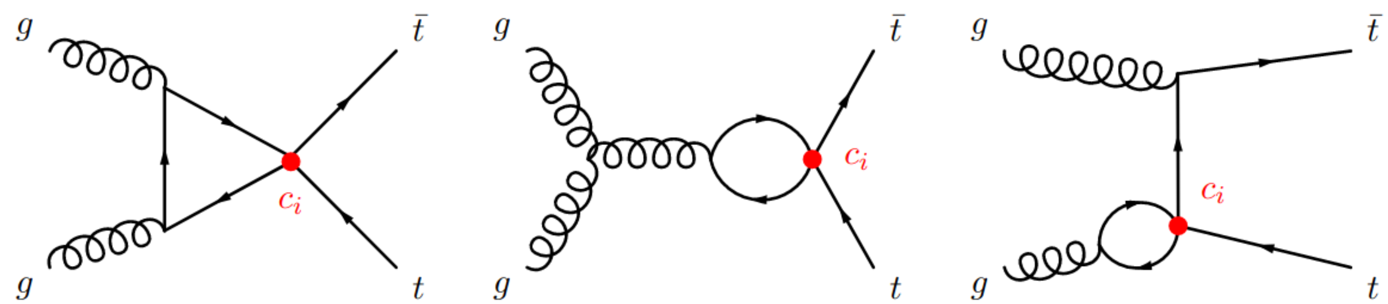

Observables are then computed as:

$$\mathrm{O}_{\mathrm{SMEFT}}\left(\frac{c_i}{\Lambda^2}\right) = \mathrm{O}_{\mathrm{SM}} + \sum_i a_i \frac{c_i}{\Lambda^2} + \sum_{ij} b_{ij} \frac{c_i c_j}{\Lambda^4}$$

Top-pair production

The four-heavy-quark operators enter through the following diagrams

Quark induced channel

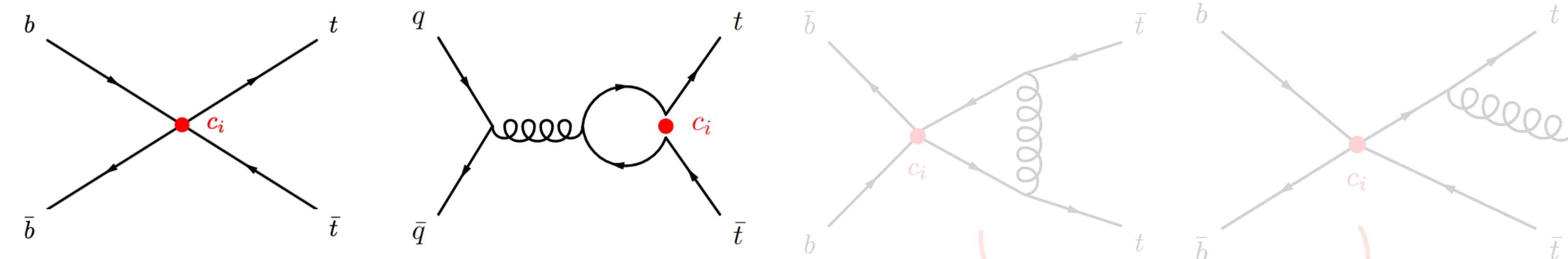

Suppressed by loop factor and bottom quark PDFs

Gluon induced channel

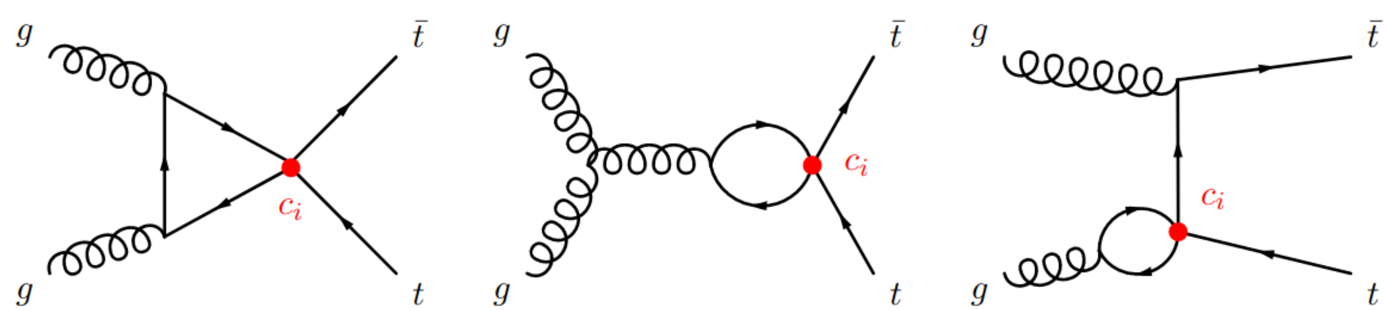

Observables are then computed as:

$$\mathrm{O}_{\mathrm{SMEFT}}\left(\frac{c_i}{\Lambda^2}\right) = \mathrm{O}_{\mathrm{SM}} + \sum_i a_i \frac{c_i}{\Lambda^2} + \sum_{ij} b_{ij} \frac{c_i c_j}{\Lambda^4}$$

The series truncated up to this order is referred as $\mathcal{O}(\Lambda^{-4})$

Interference referred as $\mathcal{O}(\Lambda^{-2})$

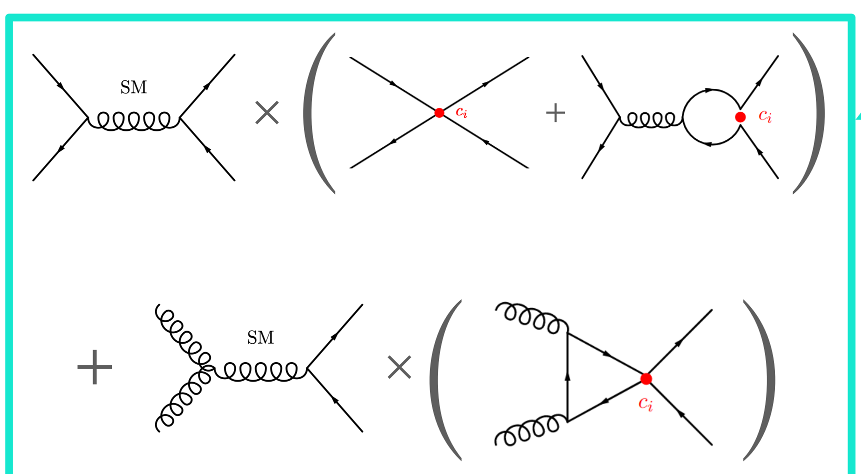

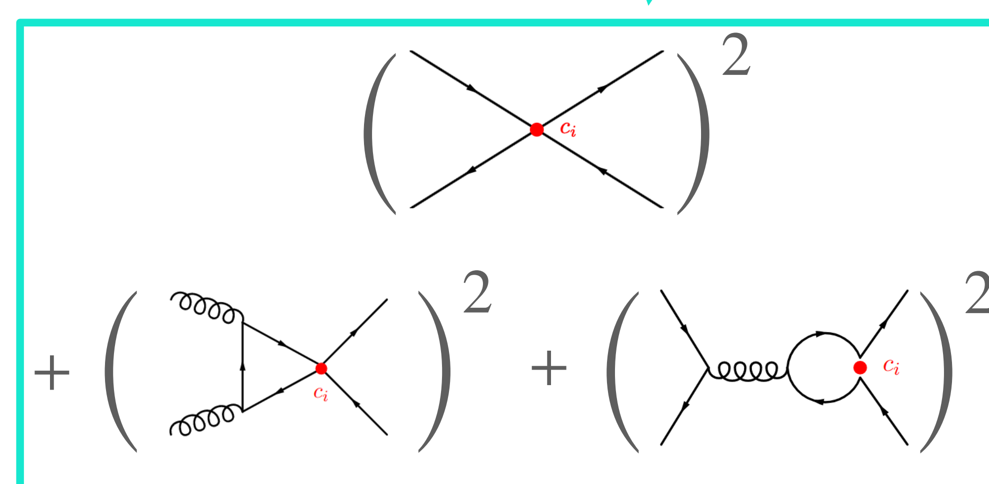

Top-pair production

The four-heavy-quark operators enter through the following diagrams

Quark induced channel

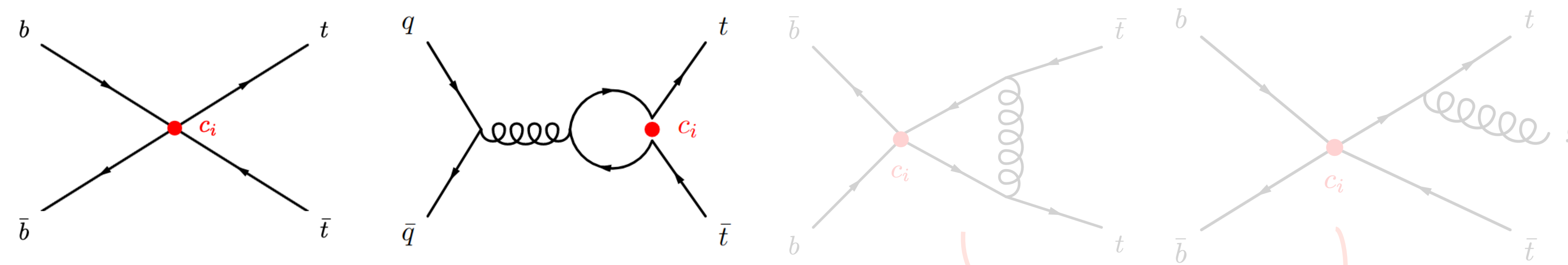

Suppressed by loop factor and bottom quark PDFs

Gluon induced channel

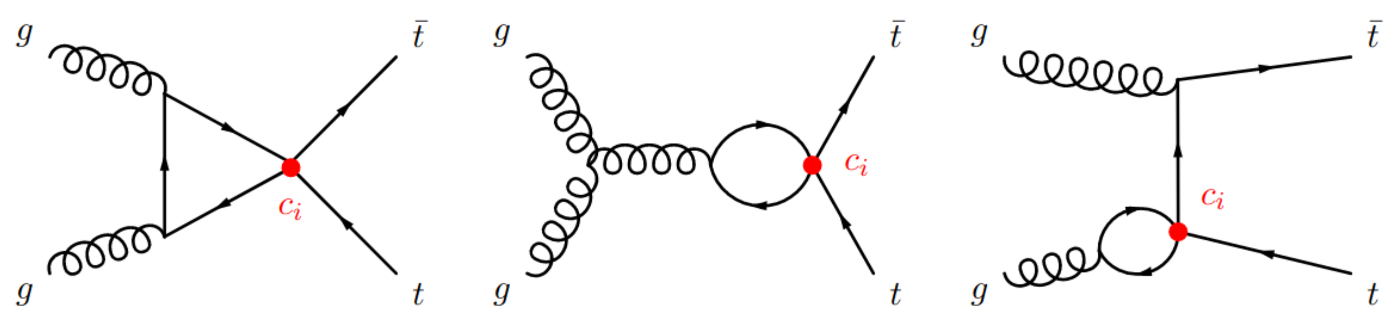

Observables are then computed as:

$$O_{\mathrm{SMEFT}}\left(\frac{c_i}{\Lambda^2}\right) = O_{\mathrm{SM}} + \sum_i a_i \frac{c_i}{\Lambda^2} + \sum_{ij} b_{ij} \frac{c_i c_j}{\Lambda^4}$$

The series truncated up to this order is referred as $\mathcal{O}(\Lambda^{-4})$

Interference referred as $\mathcal{O}(\Lambda^{-2})$

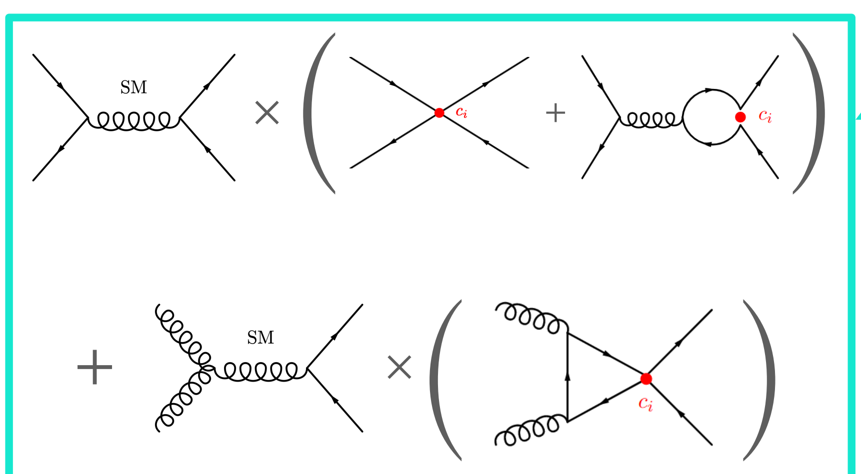

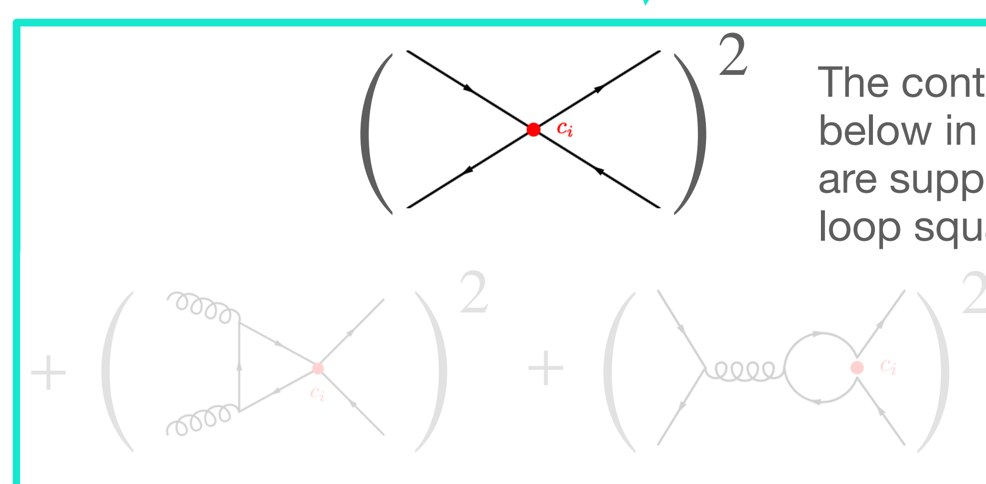

The contributions below in principle are suppressed as loop square

Top-pair production

$$K = \frac{\sigma^{(6)}_{\rm NLO}}{\sigma^{(6)}_{\rm LO}}$$

One-loop comparable to the tree-level. The latter is suppressed by PDFs.

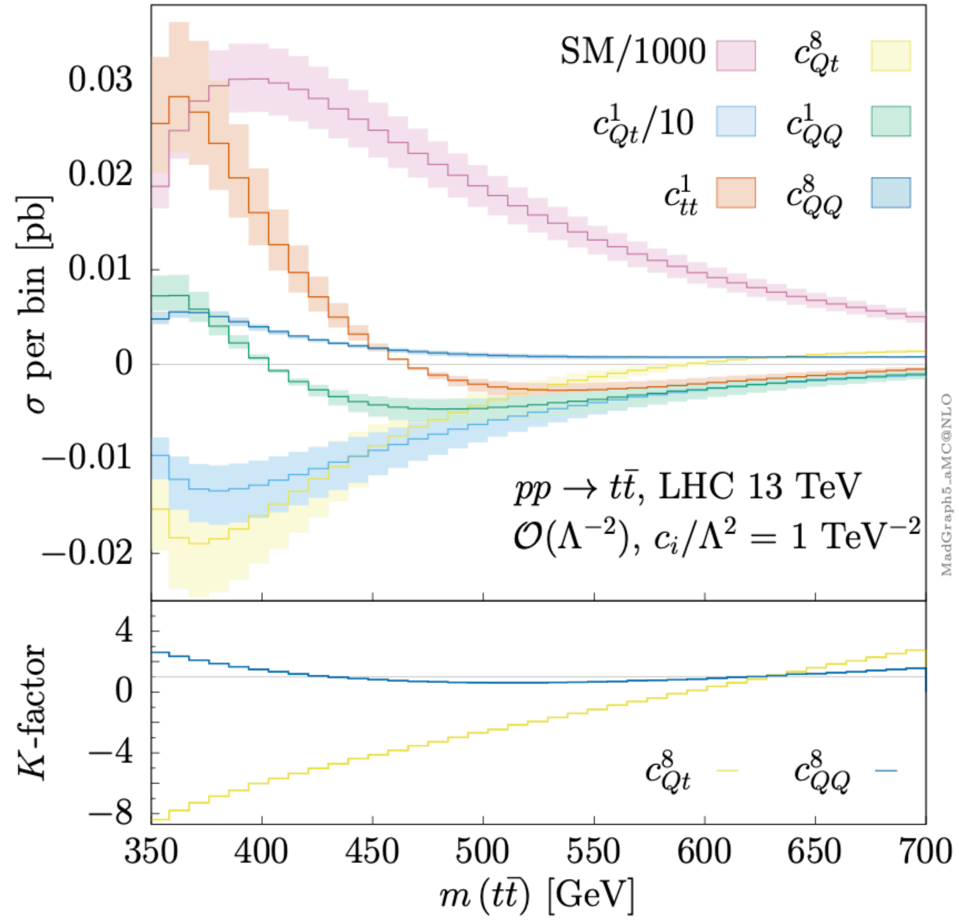

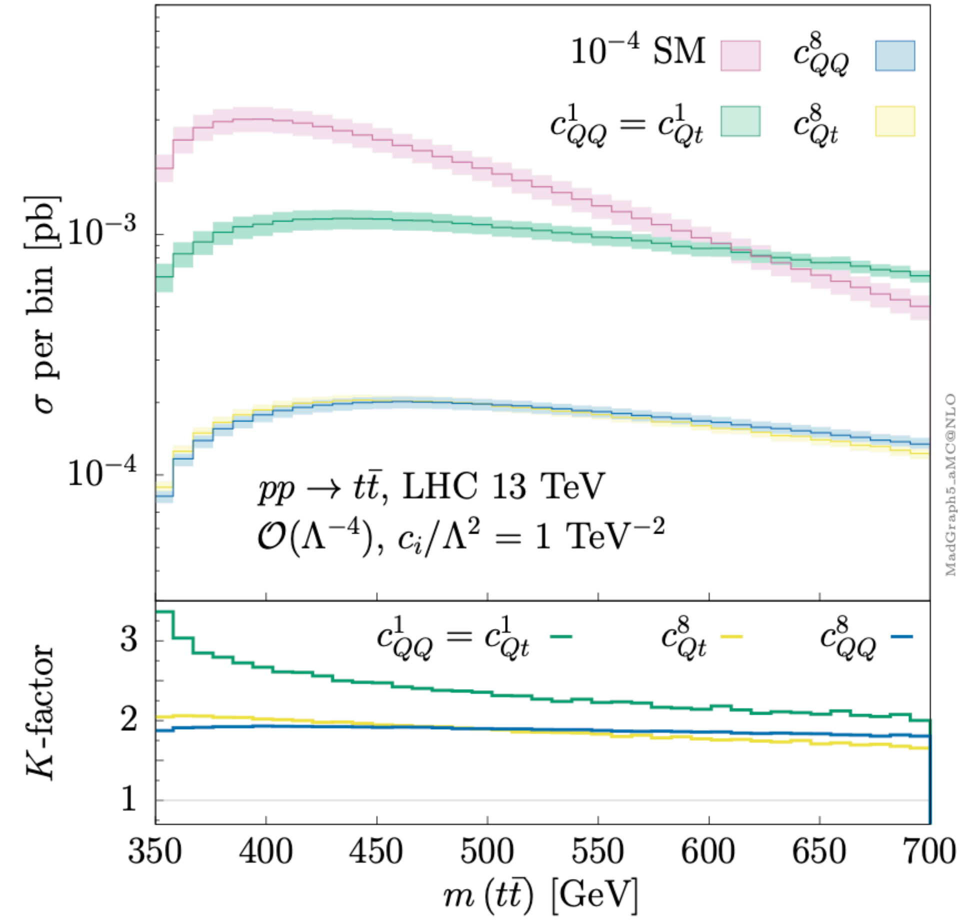

The total rates for the interference at one-loop of several of the operators suffer from phase-space cancellations.

Differential observables increase the sensitivity to NP

Change of sign understood in terms of the analytical results for the partonic differential cross-sections.

Contributions of the c^1_{Qt} are one order of magnitude larger than the other c_i. Displaced change of sign, at high-energy.

Top-pair production

Energy growth of unpolarized squared amplitude from the interference between SM and SMEFT

	$q\bar{q} \to t\bar{t}$	$gg \to t\bar{t}$
SM	$\frac{32}{9}\pi^2\alpha_s^2(1+\cos^2\theta)$	$\frac{1}{6}\pi^2\alpha_s^2\frac{(1+\cos^2\theta)(7+9\cos^2\theta)}{\sin^2\theta}$
c_{tt}^1	$\frac{8}{81}\frac{\alpha_s^2}{\Lambda^2}\hat{s}(1+\cos^2\theta)(3\log\frac{\hat{s}}{\mu^2}-2)$	$\frac{1}{6}\frac{\alpha_s^2}{\Lambda^2}m_t^2\frac{(3\cos^2\theta-13)}{\sin^2\theta}$
c_{QQ}^1	$\frac{4}{81}\frac{\alpha_s^2}{\Lambda^2}\hat{s}(1+\cos^2\theta)(3\log\frac{\hat{s}}{\mu^2}-2)$	$\frac{1}{6}\frac{\alpha_s^2}{\Lambda^2}m_t^2\frac{(3\cos^2\theta-19)}{\sin^2\theta}$
c_{QQ}^8	$\frac{2}{243}\frac{\alpha_s^2}{\Lambda^2}\hat{s}(1+\cos^2\theta)(15\log\frac{\hat{s}}{\mu^2}-28)$	$\frac{1}{36}\frac{\alpha_s^2}{\Lambda^2}m_t^2\frac{(15\cos^2\theta-41)}{\sin^2\theta}$
c_{Qt}^1	$\frac{32}{9}\frac{\alpha_s^2}{\Lambda^2}m_t^2$	$\frac{1}{6}\frac{\alpha_s^2}{\Lambda^2}m_t^2\frac{1}{\sin^2\theta}(7(\log^2\frac{\hat{s}}{m_t^2}-\pi^2)-18\cos^2\theta-19)$
c_{Qt}^8	$\frac{2}{27}\frac{\alpha_s^2}{\Lambda^2}\hat{s}(1+\cos^2\theta)(3\log\frac{\hat{s}}{\mu^2}-5)$	$\frac{1}{72}\frac{\alpha_s^2}{\Lambda^2}m_t^2\frac{1}{\sin^2\theta}(22(\log^2\frac{\hat{s}}{m_t^2}-\pi^2)+63\cos^2\theta+29)$

These are only the leading term after taking the limit $\hat{s} \gg m_t^2$.

The four-heavy-quark operators present the $\hat{s}$ factor enhancement of the two-light-two-heavy operators, but additionally they profit from a logarithmic growth, which could be used to distinguish them.

The θ-dependence is very similar to that of the SM at high-energies. Forward-backward asymmetry is not very sensitive.

Top-pair production

Energy growth of unpolarized squared amplitude from the interference between SM and SMEFT

	$q\bar{q} \to t\bar{t}$	$gg \to t\bar{t}$
SM	$\frac{32}{9}\pi^2\alpha_s^2(1+\cos^2\theta)$	$\frac{1}{6}\pi^2\alpha_s^2\frac{(1+\cos^2\theta)(7+9\cos^2\theta)}{\sin^2\theta}$
c_{tt}^1	$\frac{8}{81}\frac{\alpha_s^2}{\Lambda^2}\hat{s}(1+\cos^2\theta)(3\log\frac{\hat{s}}{\mu^2}-2)$	$\frac{1}{6}\frac{\alpha_s^2}{\Lambda^2}m_t^2\frac{(3\cos^2\theta-13)}{\sin^2\theta}$
c_{QQ}^1	$\frac{4}{81}\frac{\alpha_s^2}{\Lambda^2}\hat{s}(1+\cos^2\theta)(3\log\frac{\hat{s}}{\mu^2}-2)$	$\frac{1}{6}\frac{\alpha_s^2}{\Lambda^2}m_t^2\frac{(3\cos^2\theta-19)}{\sin^2\theta}$
c_{QQ}^8	$\frac{2}{243}\frac{\alpha_s^2}{\Lambda^2}\hat{s}(1+\cos^2\theta)(15\log\frac{\hat{s}}{\mu^2}-28)$	$\frac{1}{36}\frac{\alpha_s^2}{\Lambda^2}m_t^2\frac{(15\cos^2\theta-41)}{\sin^2\theta}$
c_{Qt}^1	$\frac{32}{9}\frac{\alpha_s^2}{\Lambda^2}m_t^2$	$\frac{1}{6}\frac{\alpha_s^2}{\Lambda^2}m_t^2\frac{1}{\sin^2\theta}(7(\log^2\frac{\hat{s}}{m_t^2}-\pi^2)-18\cos^2\theta-19)$
c_{Qt}^8	$\frac{2}{27}\frac{\alpha_s^2}{\Lambda^2}\hat{s}(1+\cos^2\theta)(3\log\frac{\hat{s}}{\mu^2}-5)$	$\frac{1}{72}\frac{\alpha_s^2}{\Lambda^2}m_t^2\frac{1}{\sin^2\theta}(22(\log^2\frac{\hat{s}}{m_t^2}-\pi^2)+63\cos^2\theta+29)$

These are only the leading term after taking the limit $\hat{s} \gg m_t^2$.

The four-heavy-quark operators present the $\hat{s}$ factor enhancement of the two-light-two-heavy operators, but additionally they profit from a logarithmic growth, which could be used to distinguish them.

The θ-dependence is very similar to that of the SM at high-energies. Forward-backward asymmetry is not very sensitive.

Spin correlations

Top-pair production

Energy growth of unpolarized squared amplitude from the interference between SM and SMEFT

	$q\bar{q} \to t\bar{t}$	$gg \to t\bar{t}$
SM	$\frac{32}{9}\pi^2\alpha_s^2(1+\cos^2\theta)$	$\frac{1}{6}\pi^2\alpha_s^2\frac{(1+\cos^2\theta)(7+9\cos^2\theta)}{\sin^2\theta}$
c_{tt}^1	$\frac{8}{81}\frac{\alpha_s^2}{\Lambda^2}\hat{s}(1+\cos^2\theta)(3\log\frac{\hat{s}}{\mu^2}-2)$	$\frac{1}{6}\frac{\alpha_s^2}{\Lambda^2}m_t^2\frac{(3\cos^2\theta-13)}{\sin^2\theta}$
c_{QQ}^1	$\frac{4}{81}\frac{\alpha_s^2}{\Lambda^2}\hat{s}(1+\cos^2\theta)(3\log\frac{\hat{s}}{\mu^2}-2)$	$\frac{1}{6}\frac{\alpha_s^2}{\Lambda^2}m_t^2\frac{(3\cos^2\theta-19)}{\sin^2\theta}$
c_{QQ}^8	$\frac{2}{243}\frac{\alpha_s^2}{\Lambda^2}\hat{s}(1+\cos^2\theta)(15\log\frac{\hat{s}}{\mu^2}-28)$	$\frac{1}{36}\frac{\alpha_s^2}{\Lambda^2}m_t^2\frac{(15\cos^2\theta-41)}{\sin^2\theta}$
c_{Qt}^1	$\frac{32}{9}\frac{\alpha_s^2}{\Lambda^2}m_t^2$	$\frac{1}{6}\frac{\alpha_s^2}{\Lambda^2}m_t^2\frac{1}{\sin^2\theta}(7(\log^2\frac{\hat{s}}{m_t^2}-\pi^2)-18\cos^2\theta-19)$
c_{Qt}^8	$\frac{2}{27}\frac{\alpha_s^2}{\Lambda^2}\hat{s}(1+\cos^2\theta)(3\log\frac{\hat{s}}{\mu^2}-5)$	$\frac{1}{72}\frac{\alpha_s^2}{\Lambda^2}m_t^2\frac{1}{\sin^2\theta}(22(\log^2\frac{\hat{s}}{m_t^2}-\pi^2)+63\cos^2\theta+29)$

Weak growth

These affects HL-LHC constrains

These are only the leading term after taking the limit $\hat{s} \gg m_t^2$.

The four-heavy-quark operators present the $\hat{s}$ factor enhancement of the two-light-two-heavy operators, but additionally they profit from a logarithmic growth, which could be used to distinguish them.

The θ-dependence is very similar to that of the SM at high-energies. Forward-backward asymmetry is not very sensitive.

Spin correlations

Datasets

Proc.	Tag	$\sqrt{s}$, $\mathcal{L}$	Final state	Observable	$n_{\rm dat}$	Ref.
$t\bar{t}$	CMS$_{tt}$-1	13 TeV, 2.3 fb^{-1}	lepton+jets	$d\sigma/dm_{t\bar{t}}$	8	[53]
	CMS$_{tt}$-2	13 TeV, 35.8 fb^{-1}	lepton+jets	$d\sigma/dm_{t\bar{t}}$	10	[26]
	CMS$_{tt}$-3	13 TeV, 2.1 fb^{-1}	dilepton	$d\sigma/dm_{t\bar{t}}$	6	[27]
	CMS$_{tt}$-4	13 TeV, 35.9 fb^{-1}	dilepton	$d\sigma/dm_{t\bar{t}}$	7	[28]
	ATLAS$_{tt}$	13 TeV, 36.1 fb^{-1}	lepton+jets	$d\sigma/dm_{t\bar{t}}$	9	[29]
	HL-LHC	14 TeV, 3 ab^{-1}	Total	$d\sigma/dm_{t\bar{t}}$	24	
$t\bar{t}t\bar{t}$	CMS$_{4t}$-1	13 TeV, 35.9 fb^{-1}	Two same-sign or multi-leptons	$\sigma_{\rm Tot}(t\bar{t}t\bar{t})$	1	[13]
	CMS$_{4t}$-2	13 TeV, 137 fb^{-1}	Two same-sign or multi-leptons	$\sigma_{\rm Tot}(t\bar{t}t\bar{t})$	1	[12]
	ATLAS$_{4t}$	13 TeV, 139 fb^{-1}	Two same-sign or multi-leptons	$\sigma_{\rm Tot}(t\bar{t}t\bar{t})$	1	[11]
	HL-LHC	14 TeV, 3 ab^{-1}	Total	$d\sigma/dm_{t\bar{t}t\bar{t}}$	11	

Statistical Analysis

We compute the observables as a function of the centre-of-mass energy and the Wilson coefficients, such that

$$\mathrm{O}_{\mathrm{SMEFT}}\left(\frac{c_i}{\Lambda^2}\right) = \mathrm{O}_{\mathrm{SM}} + \sum_i a_i \frac{c_i}{\Lambda^2} + \sum_{ij} b_{ij} \frac{c_i c_j}{\Lambda^4},$$

The exclusion regions are computed through a chi-squared distribution analysis

$$\chi_i^2\left(\frac{c_i}{\Lambda^2}\right) = \sum_{\mathrm{Bins}} \frac{\left(\mathrm{O}_{\mathrm{SMEFT}}\left(\frac{c_i}{\Lambda^2}\right) - \mathrm{O}_{\mathrm{Exp}}\right)^2}{(\delta \mathrm{O})^2}, \qquad \chi^2 = \sum_i \chi_i^2\left(\frac{c_i}{\Lambda^2}\right).$$

For the projected sensitivity, the uncertainties are parametrised as

$$\delta \mathrm{O}_n = \sqrt{(\delta \mathrm{O}_n)^2_{\mathrm{stat}} + (\delta \mathrm{O}_n)^2_{\mathrm{syst}}} = \sqrt{\frac{\sigma_n^{\mathrm{SM}}}{\mathcal{L}} + \alpha^2 (\sigma_n^{\mathrm{SM}})^2},$$

The results that follow were obtained using MadGraph5_aMC@NLO and SMEFT@NLO.

[Degrande et al., 2020]

Bounds on 4-heavy quark op.

			CMS$_{tt}$-1	CMS$_{tt}$-2	CMS$_{tt}$-3	CMS$_{tt}$-4	ATLAS$_{tt}$	Combined
c^1_{tt}	Ind.	$\mathcal{O}(\Lambda^{-2})$	$[-148, 64.4]$	$[-58.9, 0.99]$	$[-129, 332]$	$[-56.4, -0.81]$	$[-26.4, 52.2]$	$[-28.1, 7.16]$
		$\mathcal{O}(\Lambda^{-4})$	$[-148, 64.4]$	$[-58.9, 0.99]$	$[-129, 332]$	$[-56.4, -0.81]$	$[-26.4, 52.2]$	$[-28.1, 7.16]$
	Marg.	$\mathcal{O}(\Lambda^{-4})$	$[-122, 3.22]$	$[-50.8, -10.8] \cup [4.55, 255]$	-	-	$[-232, 129]$	$[-48.0, 2.83]$
c^1_{QQ}	Ind.	$\mathcal{O}(\Lambda^{-2})$	$[-292, 139]$	$[-107, 2.17]$	$[-335, 462]$	$[-109, -1.66]$	$[94.3, -51.3]$	$[-51.7, 14.9]$
		$\mathcal{O}(\Lambda^{-4})$	$[-18.2, 16.2]$	$[-3.04, 1.27]$	$[-21.4, 21.1]$	-	$[-19.7, 18.1]$	$[-5.72, 4.29]$
	Marg.	$\mathcal{O}(\Lambda^{-4})$	$[-12.7, 13.1]$	$[-15.3, 12.1]$	-	-	$[-26.5, 24.0]$	$[-8.05, 4.95]$
c^8_{QQ}	Ind.	$\mathcal{O}(\Lambda^{-2})$	$[-323, 126]$	$[-157, 1.74]$	$[-575, 334]$	$[-119, -2.53]$	$[-60.1, 105]$	$[-66.9, 15.0]$
		$\mathcal{O}(\Lambda^{-4})$	$[-43.0, 32.1]$	$[-11.9, 1.52]$	$[-48.9, 43.1]$	-	$[-40.2, 29.2]$	$[-16.1, 7.90]$
	Marg.	$\mathcal{O}(\Lambda^{-4})$	$[-31.5, 26.7]$	$[-316, 163]$	-	-	$[-75.2, 68.8]$	$[-18.7, 14.8]$
c^1_{Qt}	Ind.	$\mathcal{O}(\Lambda^{-2})$	$[-53.7, 78.8]$	$[-3.23, 11.4]$	$[-451, 28.0]$	-	$[-33.2, 29.0]$	$[-11.4, 12.7]$
		$\mathcal{O}(\Lambda^{-4})$	$[-15.9, 17.7]$	$[-1.52, 2.32]$	$[-30.4, 14.8]$	-	$[-20.7, 12.3]$	$[-4.94, 4.80]$
	Marg.	$\mathcal{O}(\Lambda^{-4})$	$[-6.79, 18.2]$	$[-50.3, 30.2]$	-	-	$[-43.8, 24.7]$	$[-6.33, 7.24]$
c^8_{Qt}	Ind.	$\mathcal{O}(\Lambda^{-2})$	$[-177, 69.5]$	$[-100, 0.88]$	$[-322, 64.3]$	$[-95.8, -0.77]$	$[-32.3, 44.9]$	$[-44.6, 5.92]$
		$\mathcal{O}(\Lambda^{-4})$	$[-55.5, 31.1]$	$[-26.0, 0.85]$	$[-72.8, 34.2]$	$[-27.3, -0.79]$	$[-59.7, 25.7]$	$[-31.4, 5.02]$
	Marg.	$\mathcal{O}(\Lambda^{-4})$	$[-35.6, 25.2]$	$[-142, -6.50] \cup [2.21, 82.5]$	-	-	$[-100, 58.2]$	$[-23.7, 1.77]$

Table 5: The 95% CL bounds (assuming $\Lambda = 1$ TeV) for the coefficients of the four-heavy-quark operators in the process $pp \to t\bar{t}$ individual and marginalized. The intervals are presented for the different datasets introduced in Table 4. The missing entries correspond to cases where the SM does not provide a good fit to the data. Notice that $\mathcal{O}(\Lambda^{-4})$ includes terms of the order $\mathcal{O}(\Lambda^{-2})$ (see Eq. (4.3))

Bounds on 4-heavy quark op.

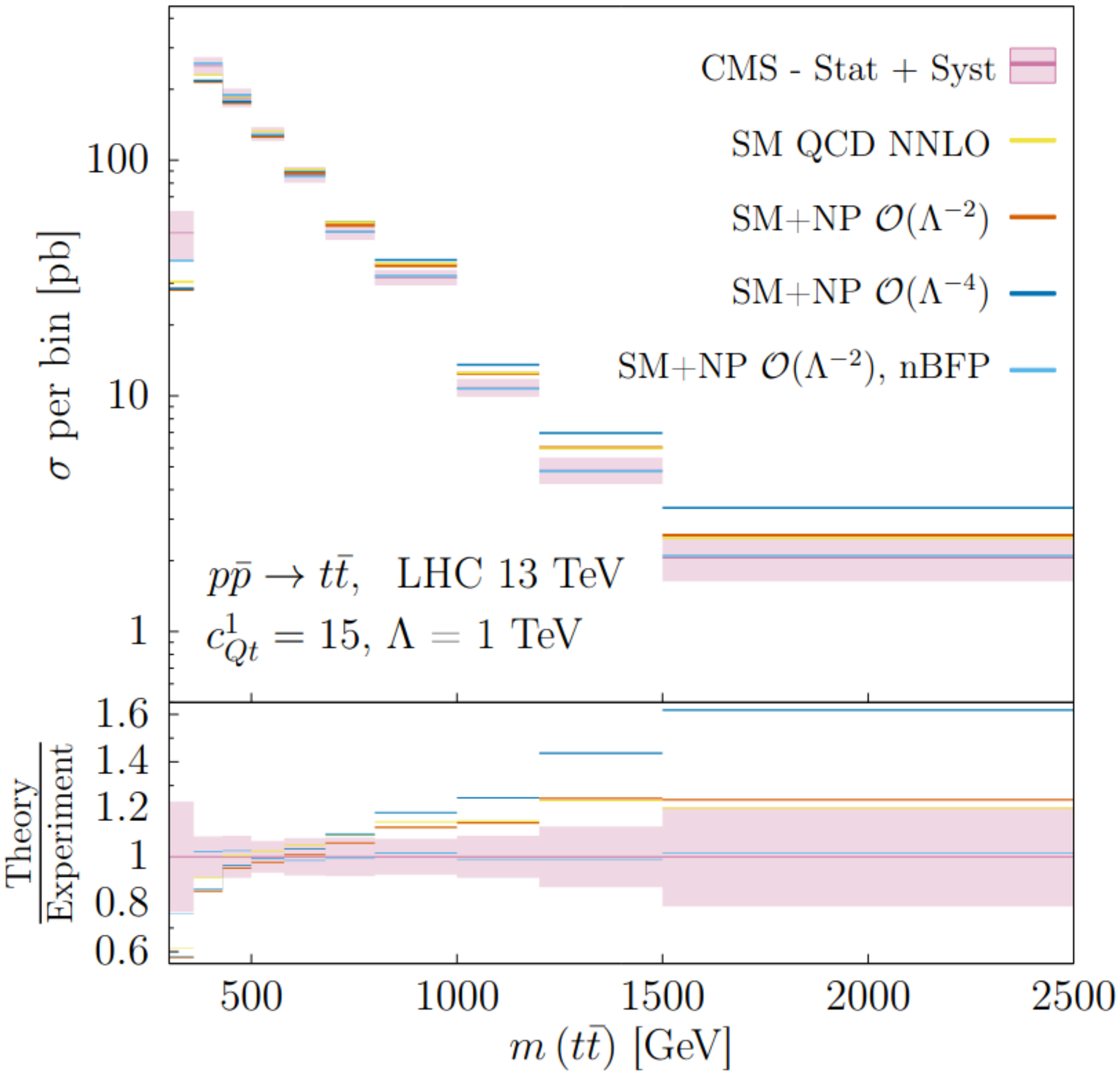

Fit to the invariant mass distribution measured by CMS in the lepton+jets channel with a luminosity of 35.8 fb^{-1}.

The best fit point (BFP) found at

$$c^1_{tt} = 116, \qquad c^1_{Qt} = -64.9, \qquad c^1_{QQ} = 484\,(150),$$
$$c^8_{Qt} = 164\,(150), \qquad c^8_{QQ} = -1113\,(-150),$$

To illustrate the capability of the effective operators to fit data we show the invariant mass distribution near the BFP.

In the diagonal basis the BFP is

$$c_1 = -16.6, \quad c_2 = 0.944, \quad c_3 = -128, \quad c_4 = 123 \quad c_5 = 2038.$$

Bounds on 4-heavy quark op.

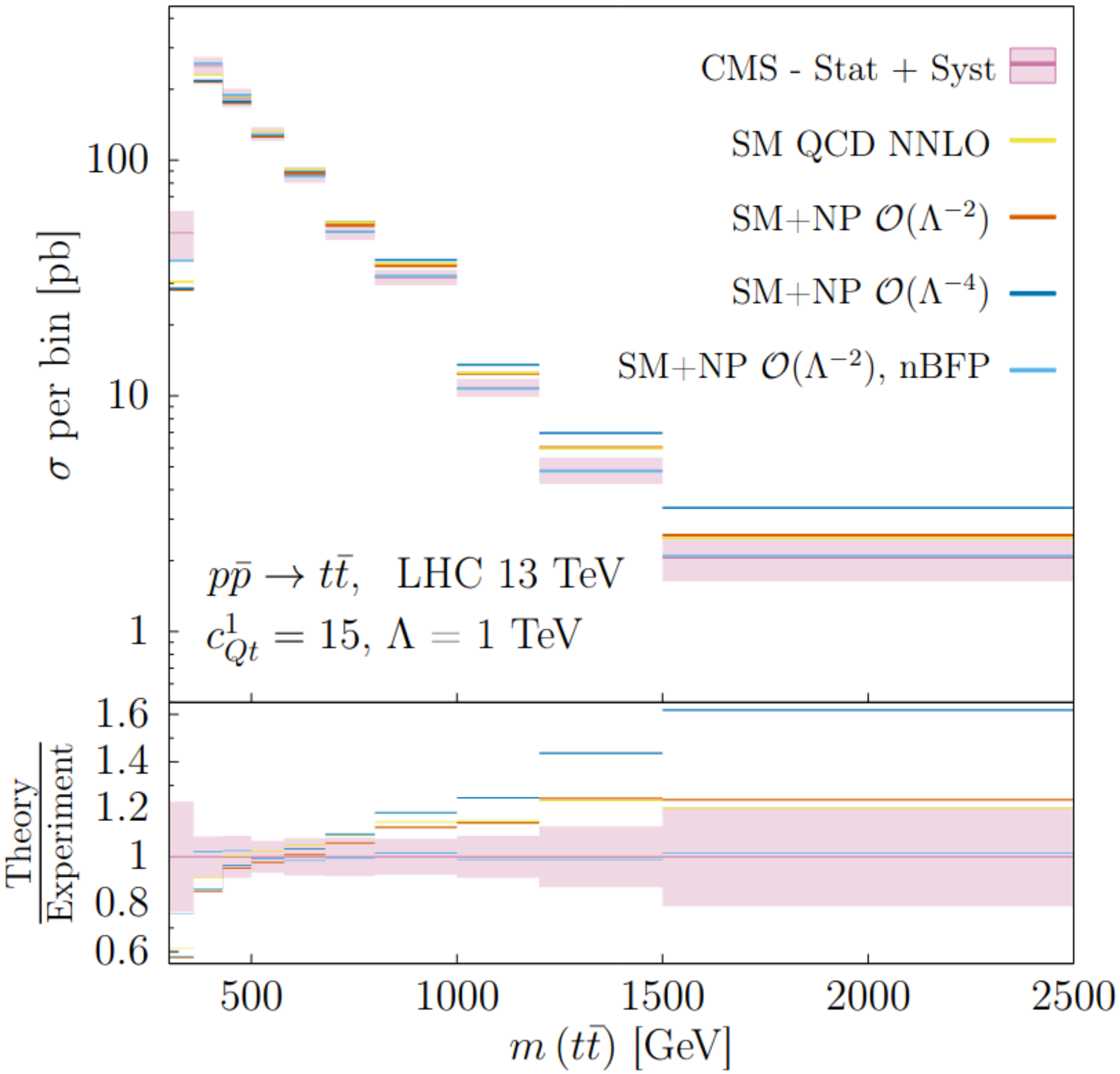

Tension in the first bin between SM and measurements.

EFT effects bring the theoretical prediction of the first bin very close to the error band.

Fit to the invariant mass distribution measured by CMS in the lepton+jets channel with a luminosity of 35.8 fb^{-1}.

The best fit point (BFP) found at

$$c^1_{tt} = 116, \qquad c^1_{Qt} = -64.9, \qquad c^1_{QQ} = 484\,(150),$$
$$c^8_{Qt} = 164\,(150), \qquad c^8_{QQ} = -1113\,(-150),$$

To illustrate the capability of the effective operators to fit data we show the invariant mass distribution near the BFP.

In the diagonal basis the BFP is

$$c_1 = -16.6, \quad c_2 = 0.944, \quad c_3 = -128, \quad c_4 = 123 \quad c_5 = 2038.$$

Bounds on 4-heavy quark op.

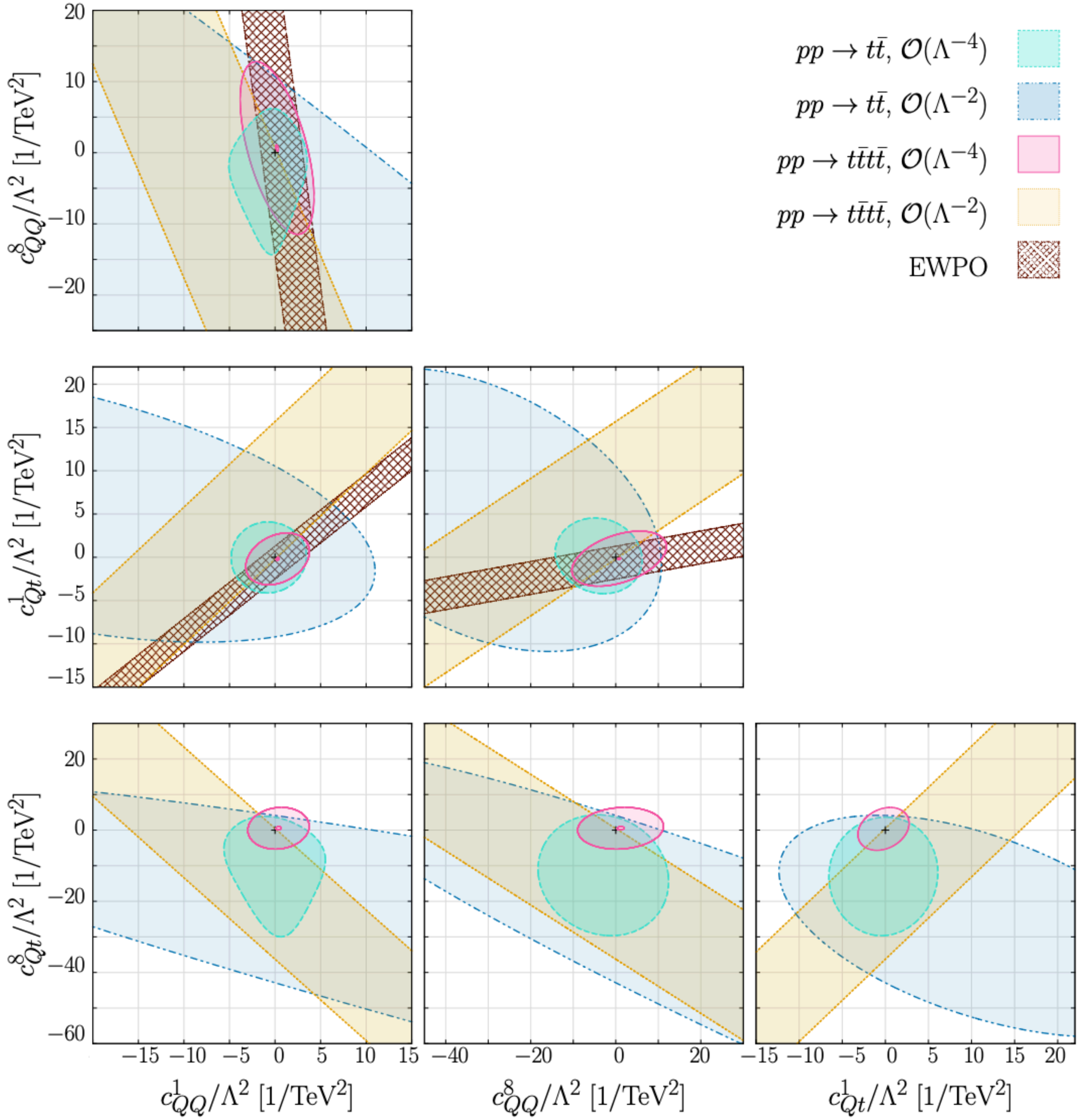

Exclusion regions at 95% CL.
The points outside the regions are excluded.

For these bounds, only datasets from different final state and collaboration were combined.

Bounds for the $t\bar{t}t\bar{t}$ are presented as planes, which is a consequence of only having two data points in the fit.

Bounds on 4-heavy quark op.

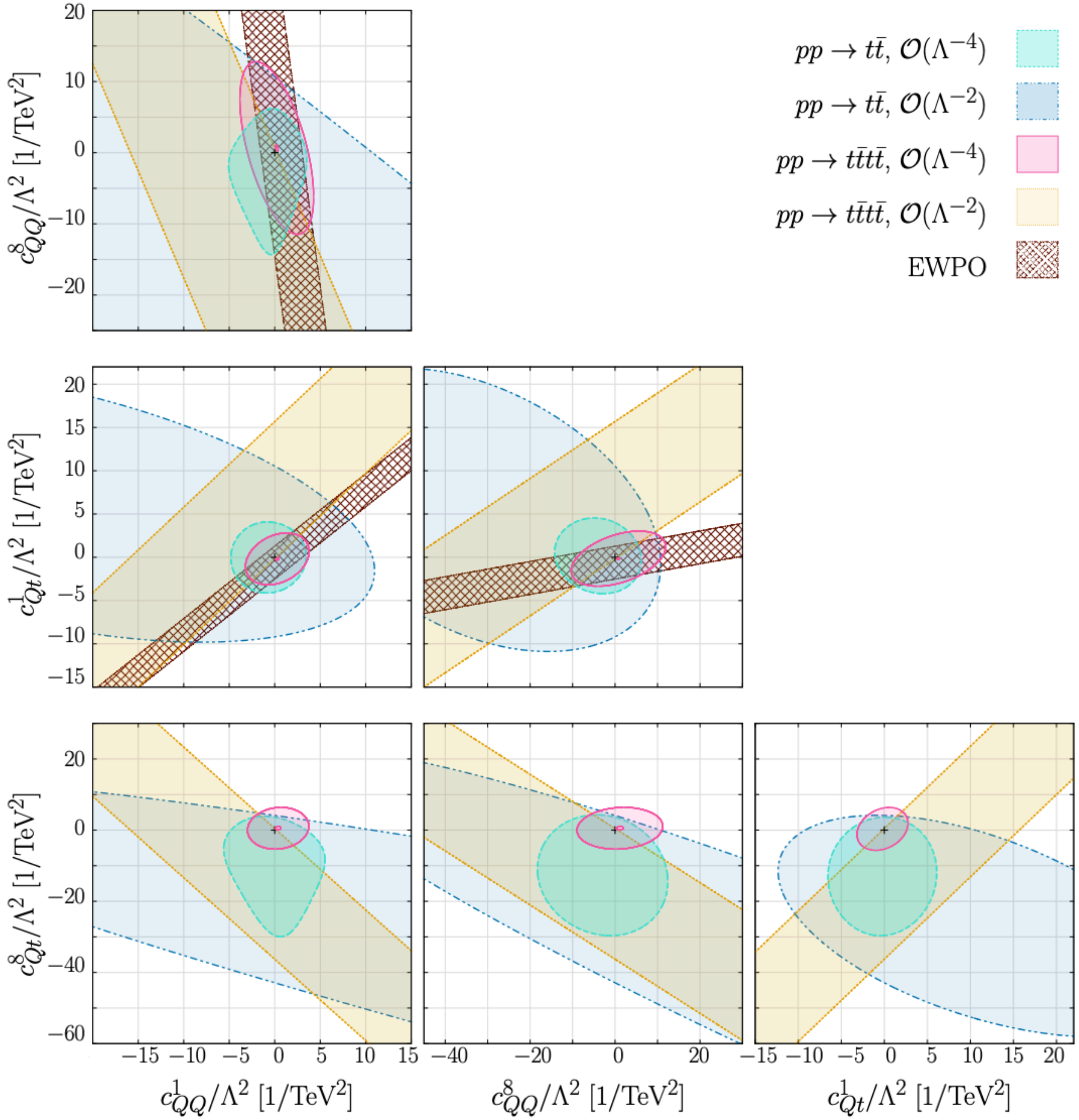

Exclusion regions at 95% CL. The points outside the regions are excluded.

For these bounds, only datasets from different final state and collaboration were combined.

Bounds for the $t\bar{t}t\bar{t}$ are presented as planes, which is a consequence of only having two data points in the fit.

Bounds from Electroweak precision observables (EWPO):

$$\Gamma_Z,\ \sigma_{\rm h},\ R_l,\ R_b,\ R_c,\ A_b,\ A_{b,\rm FB}$$

Bounds from Higgs processes seem to be more stable when terms of order $\mathcal{O}(\Lambda^{-4})$ are included. Not shown here.

Bounds on 4-heavy quark op.

Regions for the c_{tt}^1 case.

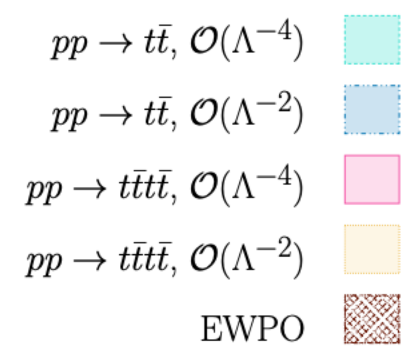

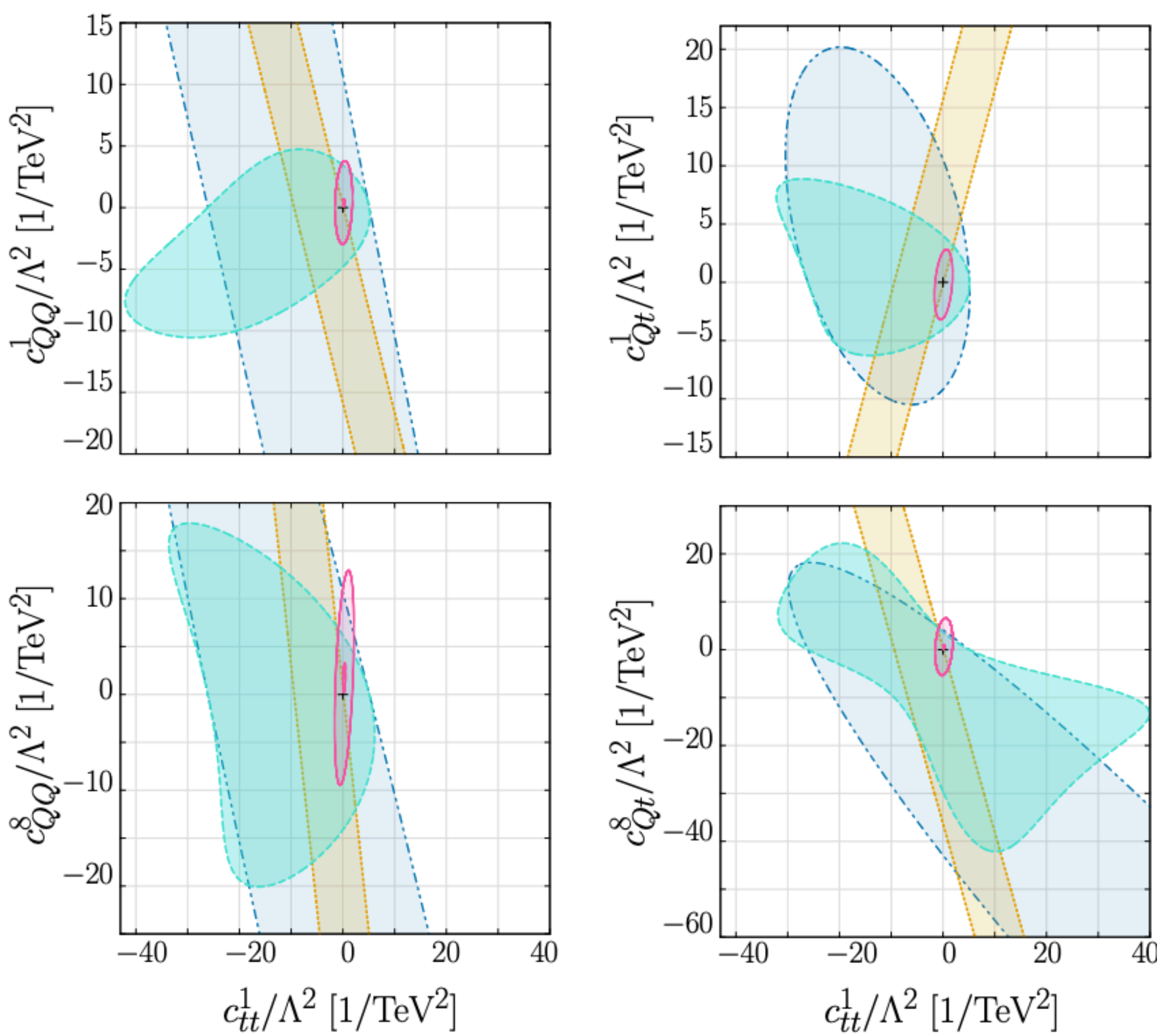

Bounds from the interference are complementary between the two processes.

Bounds from $t\bar{t}t\bar{t}$ in the quadratic case are much more stringent than the corresponding ones from $t\bar{t}$ production.

The $t\bar{t}t\bar{t}$ process is sensitive the most to c_{tt}^1.

HL-LHC

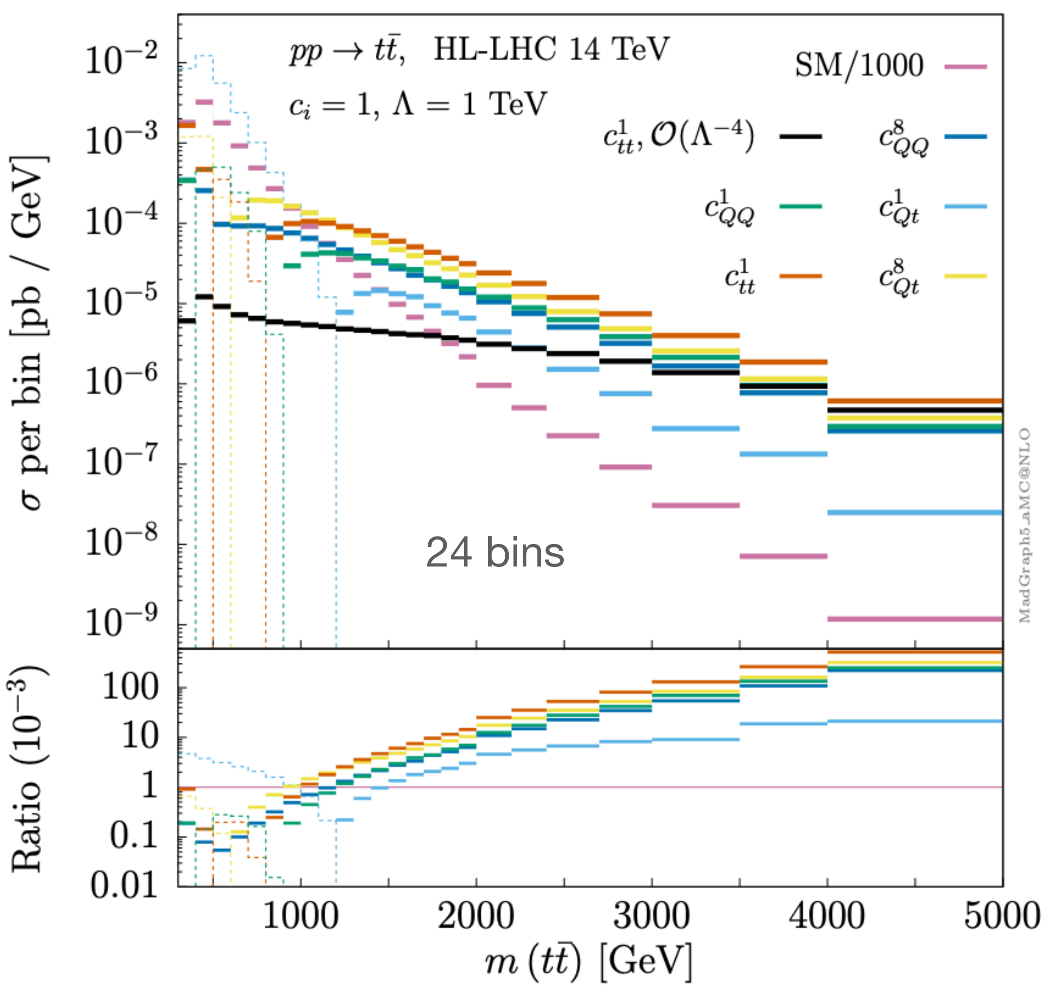

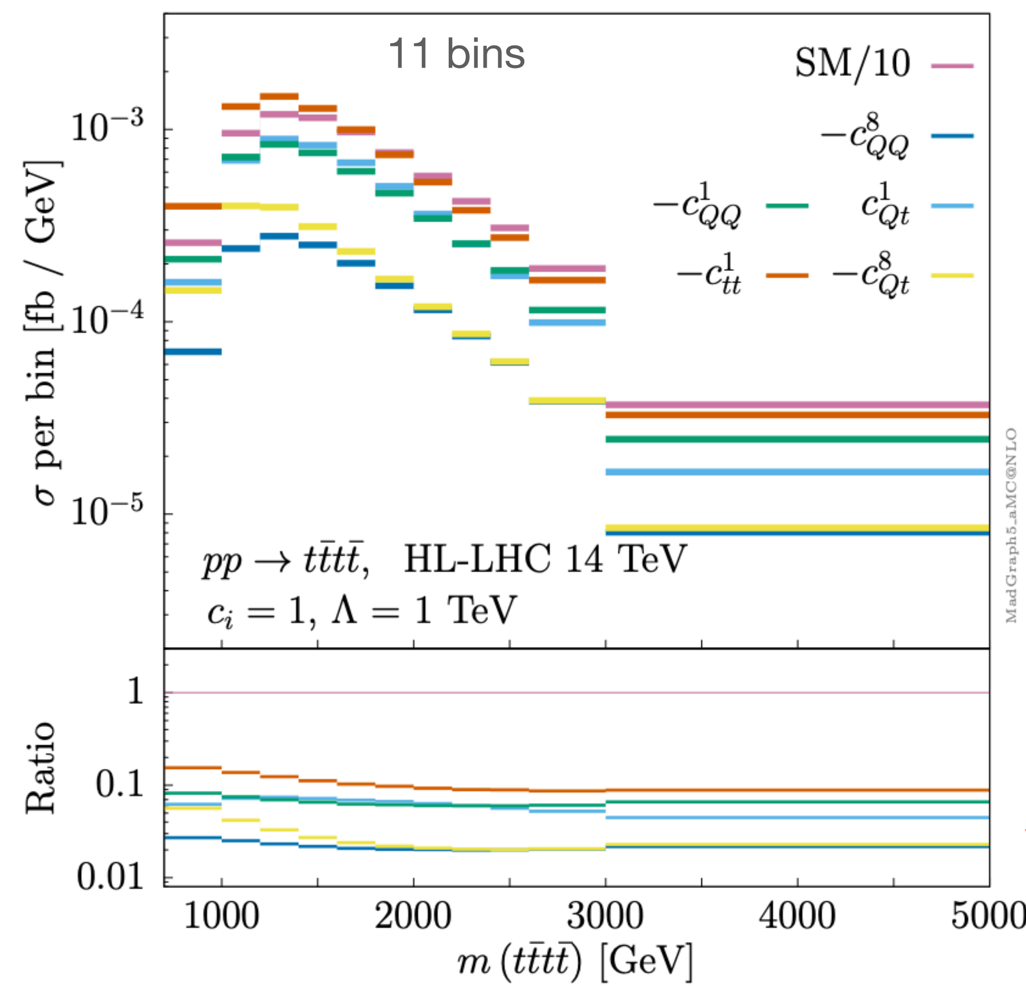

The $t\bar{t}t\bar{t}$ tends to constraint the same direction as all of the distributions are very similar.

At order $\mathcal{O}(\Lambda^{-2})$ the $t\bar{t}t\bar{t}$ seems to be more under control at the high-energy bins than the $t\bar{t}$.

No improvement in the bounds when including the bin centred at 4 TeV, since in the high-energy region the distributions are SM-like. This changes with $\mathcal{O}(\Lambda^{-4})$ terms.

HL-LHC

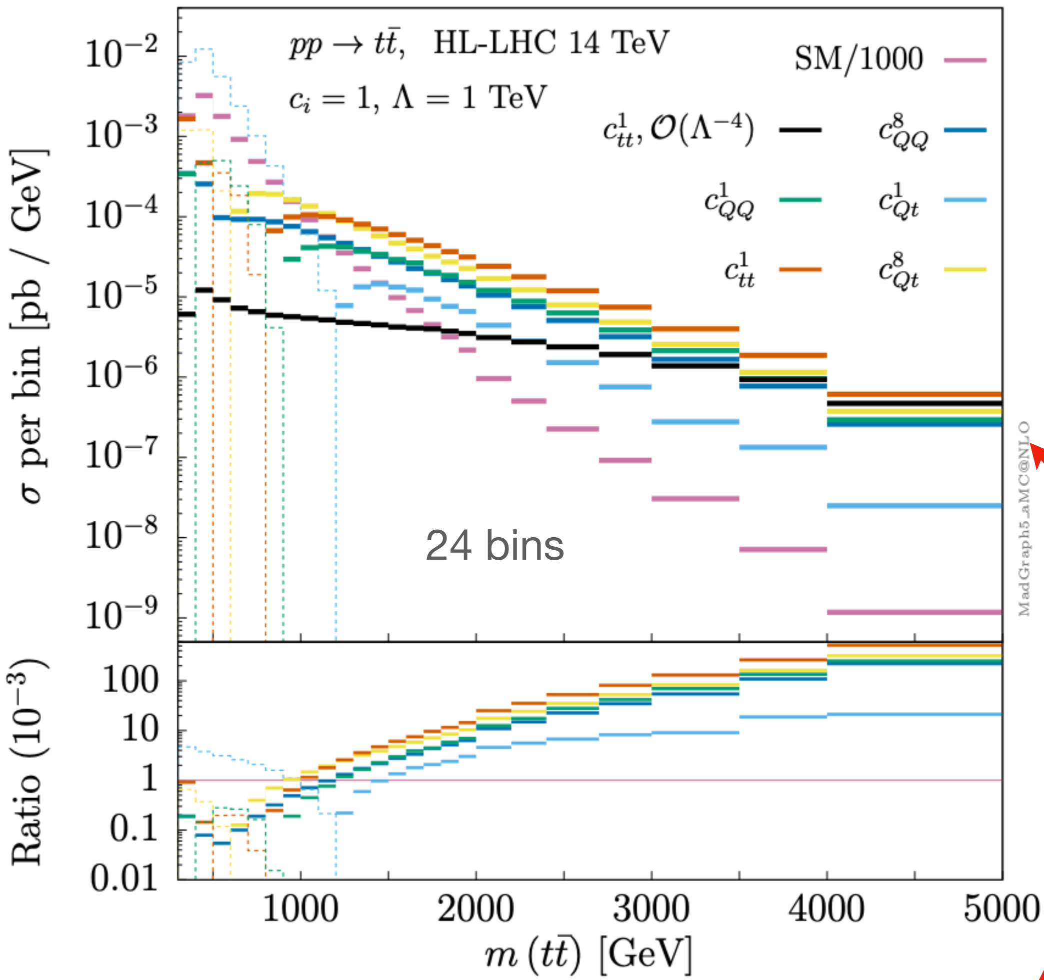

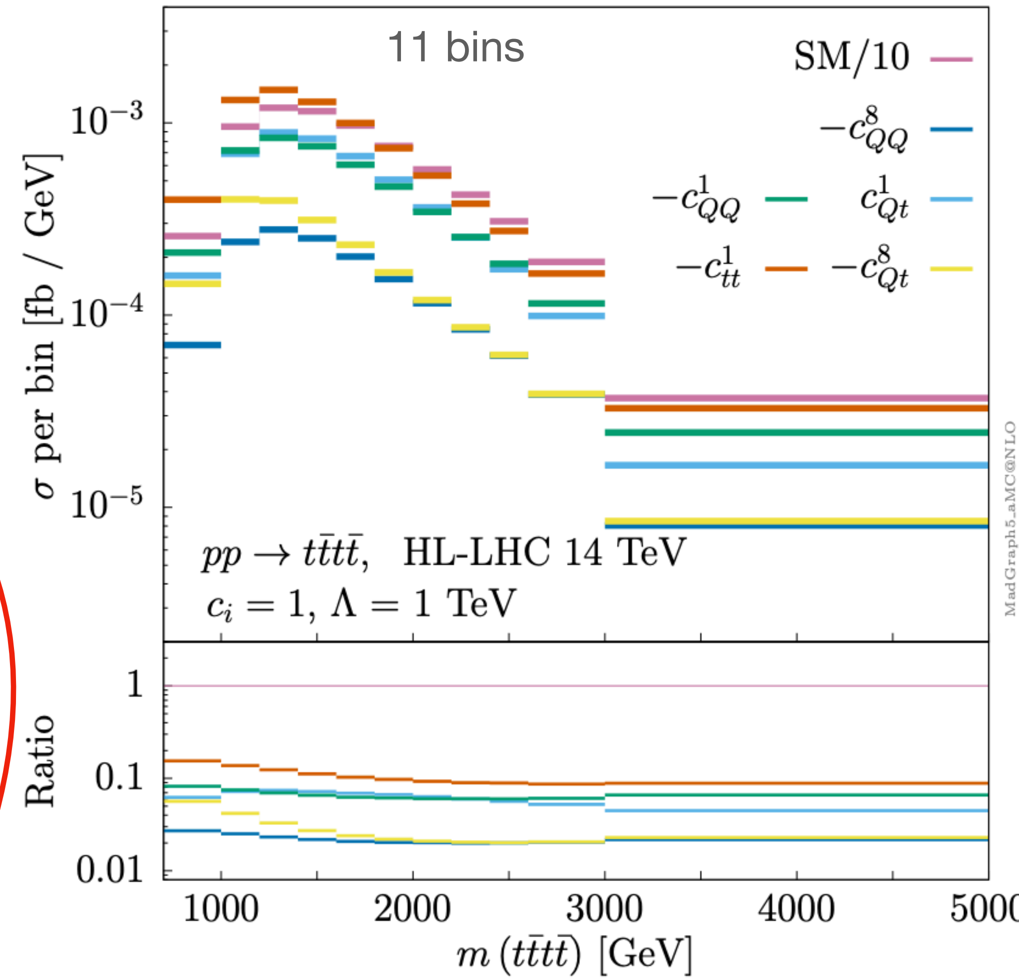

The $t\bar{t}t\bar{t}$ tends to constraint the same direction as all of the distributions are very similar.

At order $\mathcal{O}(\Lambda^{-2})$ the $t\bar{t}t\bar{t}$ seems to be more under control at the high-energy bins than the $t\bar{t}$.

Hard to distinguish the operators in the high-energy region. The particular behaviour of the c^1_{Qt} operator is due to the quark-induced channel.

No improvement in the bounds when including the bin centred at 4 TeV, since in the high-energy region the distributions are SM-like. This changes with $\mathcal{O}(\Lambda^{-4})$ terms.

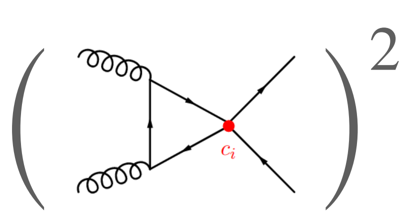

Loop-square contributions are the full corrections of order $\alpha_s^2\Lambda^{-4}$ for the $\mathcal{O}^{(1)}_{tt}$ operator. At enough high-energies, these contributions have a similar magnitude as the corresponding interference ones.

HL-LHC

Marginalized 95% CL bounds (Λ = 1 TeV) for the interference given by the coefficients of the four-heavy-quark operators in the diagonal basis of the processes $pp \to t\bar{t}$ and $pp \to t\bar{t}t\bar{t}$.

c_i	Cut	$pp \to t\bar{t}$	$pp \to t\bar{t}t\bar{t}$	$t\bar{t} + t\bar{t}t\bar{t}$
c_1	$m_{\text{Tot.}} < 5$ TeV	$[-0.35, 0.35]$	$[-1.46, 1.46]$	$[-0.42, 0.42]$
	$m_{\text{Tot.}} < 3$ TeV	$[-1.71, 1.71]$	$[-1.42, 1.42]$	$[-1.71, 1.71]$
c_2	$m_{\text{Tot.}} < 5$ TeV	$[-17.6, 17.6]$	$[-18.6, 18.6]$	$[-4.95, 4.95]$
	$m_{\text{Tot.}} < 3$ TeV	$[-29.8, 29.8]$	$[-17.5, 17.5]$	$[-5.36, 5.36]$
c_3	$m_{\text{Tot.}} < 5$ TeV	$[-39.6, 39.6]$	$[-37.5, 37.5]$	$[-26.3, 26.3]$
	$m_{\text{Tot.}} < 3$ TeV	$[-85.5, 85.5]$	$[-55.5, 55.5]$	$[-61.6, 61.6]$
c_4	$m_{\text{Tot.}} < 5$ TeV	$[-62.1, 62.1]$	$[-477, 477]$	$[-63.3, 63.3]$
	$m_{\text{Tot.}} < 3$ TeV	$[-289, 289]$	$[-509, 509]$	$[-68.9, 68.9]$
c_5	$m_{\text{Tot.}} < 5$ TeV	$[-403, 403]$	$[-1785, 1785]$	$[-74.9, 74.9]$
	$m_{\text{Tot.}} < 3$ TeV	$[-727, 727]$	$[-2213, 2213]$	$[-217, 217]$

Summary & outlook

Main message:

The top-pair production offers the possibility to probe dimension-6 operators involving only the bottom and top quark, an often overlooked process when constraining such operators.

- Global analyses that consider the four-top production to bound the four-heavy-quark operators will benefit from considering the top-pair.
- We find that both processes are in the same ballpark in terms of the EFT validity. Push bounds one order of magnitude to be safe.
- The analytic computation of the SMEFT predictions lead to the identification of a bug in MadGraph5_aMC@NLO. For the first time, a full validation of SMEFT one-loop computations in MadGraph5_aMC@NLO.

Summary & outlook

Main message:

The top-pair production offers the possibility to probe dimension-6 operators involving only the bottom and top quark, an often overlooked process when constraining such operators.

- Global analyses that consider the four-top production to bound the four-heavy-quark operators will benefit from considering the top-pair.
- We find that both processes are in the same ballpark in terms of the EFT validity. Push bounds one order of magnitude to be safe.
- The analytic computation of the SMEFT predictions lead to the identification of a bug in MadGraph5_aMC@NLO. For the first time, a full validation of SMEFT one-loop computations in MadGraph5_aMC@NLO.

- More optimized observables are required to improve the constraints. Look at spin correlations.
- Investigate more the phase-space cancellations in the four-top production.

Back up

		$pp \to t\bar{t}$			$pp \to t\bar{t}t\bar{t}$			$t\bar{t} + t\bar{t}t\bar{t}$
c_i	Cut	Individual $\mathcal{O}(\Lambda^{-2})$	Individual $\mathcal{O}(\Lambda^{-4})$	Marginalized $\mathcal{O}(\Lambda^{-4})$	Individual $\mathcal{O}(\Lambda^{-2})$	Individual $\mathcal{O}(\Lambda^{-4})$	Marginalized $\mathcal{O}(\Lambda^{-4})$	Marginalized $\mathcal{O}(\Lambda^{-4})$
c^1_{tt}	$m_{\text{Tot.}} < 5$ TeV	$[-0.51, 0.51]$	$[-0.51, 0.51]$	$[-11.3, 10.6]$	$[-2.37, 2.37]$	$[-0.55, 0.66]$	$[-0.26, 0.33]$	$[-0.71, 0.80]$
	$m_{\text{Tot.}} < 3$ TeV	$[-2.58, 2.58]$	$[-2.58, 2.58]$	$[-38.1, 13.2]$	$[-2.35, 2.35]$	$[-0.62, 0.78]$	$[-0.30, 0.40]$	$[-0.82, 0.94]$
c^1_{QQ}	$m_{\text{Tot.}} < 5$ TeV	$[-1.02, 1.02]$	$[-1.11, 0.96]$	$[-5.82, 5.38]$	$[-3.91, 3.91]$	$[-1.07, 1.35]$	$[-2.30, 2.35]$	$[-2.50, 3.94]$
	$m_{\text{Tot.}} < 3$ TeV	$[-5.0, 5.0]$	$[-7.71, 3.07]$	$[-10.3, 11.4]$	$[-3.95, 3.95]$	$[-1.21, 1.61]$	$[-2.37, 2.44]$	$[-3.17, 5.08]$
c^8_{QQ}	$m_{\text{Tot.}} < 5$ TeV	$[-1.21, 1.21]$	$[-1.24, 1.18]$	$[-13.1, 12.7]$	$[-11.8, 11.8]$	$[-3.22, 4.07]$	$[-6.88, 7.14]$	$[-9.87, 5.47]$
	$m_{\text{Tot.}} < 3$ TeV	$[-6.01, 6.01]$	$[-21.1, 4.74]$	$[-26.3, 28.7]$	$[-11.9, 11.9]$	$[-3.62, 4.82]$	$[-7.05, 7.35]$	$[-15.2, 7.73]$
c^1_{Qt}	$m_{\text{Tot.}} < 5$ TeV	$[-9.03, 9.03]$	$[-4.24, 2.92]$	$[-6.45, 5.39]$	$[-4.07, 4.07]$	$[-1.12, 0.94]$	$[-0.55, 0.44]$	$[-1.36, 1.21]$
	$m_{\text{Tot.}} < 3$ TeV	$[-17.7, 17.7]$	$[-5.44, 4.31]$	$[-10.8, 10.2]$	$[-4.0, 4.0]$	$[-1.35, 1.06]$	$[-0.70, 0.51]$	$[-1.63, 1.41]$
c^8_{Qt}	$m_{\text{Tot.}} < 5$ TeV	$[-0.82, 0.82]$	$[-0.82, -0.82]$	$[-16.4, 12.0]$	$[-8.58, 8.58]$	$[-1.96, 2.29]$	$[-0.91, 1.12]$	$[-2.50, 2.56]$
	$m_{\text{Tot.}} < 3$ TeV	$[-3.86, 3.86]$	$[-4.21, 3.61]$	$[-27.7, 20.8]$	$[-8.47, 8.47]$	$[-2.23, 2.71]$	$[-1.06, 1.32]$	$[-2.91, 3.04]$

Table 8: The 95% confidence level bounds (assuming $\Lambda = 1$ TeV) for the coefficients of the four-heavy-quark operators in the processes $pp \to t\bar{t}$ and $pp \to t\bar{t}t\bar{t}$ at the HL-LHC with $\sqrt{s} = 14$ TeV. The intervals are presented for two different cuts in the invariant-mass distribution.